Endocytic SNAREs are involved in optimal *Coxiella burnetii* vacuole development

Emanuel Martín Campoy, María Eugenia Mansilla and María Isabel Colombo*

Laboratorio de Biología Celular y Molecular- Instituto de Histología y Embriología (IHEM), Facultad de Ciencias Médicas, Universidad Nacional de Cuyo-CONICET, Mendoza, Argentina.

Summary

***Coxiella burnetii* is a Gram-negative intracellular bacterium. As previously described, both the endocytic and the autophagic pathways contribute to the maturation of *Coxiella* replicative vacuoles (CRVs). The large CRVs share the properties of both phagolysosomal and autophagolysosomal compartments. Vamp3, Vamp7 and Vamp8 are v-SNAREs involved in the endocytic pathway which participate mainly in the fusion between endosomes and lysosomes. In the present study we observed that Vamp7 interacts with *C. burnetii* at different infection times (1 h–48 h p.i.). We have determined that a truncated mutant of Vamp7 (Vamp7 NT) and a siRNA against this SNARE protein affects the optimal development of CRVs, suggesting that Vamp7 mediates fusion events that are required for the biogenesis of CRVs. Indeed, we have observed that overexpression of Vamp7 NT inhibited the heterotypic fusion with lysosomes and the homotypic fusion between individual *Coxiella* phagosomes and CRVs. Moreover, we have detected in the vacuole membrane, at different infection times, the Vamp7 partners (Vti1a and Vti1b). Interestingly, treatment with chloramphenicol reduced the colocalization between *C. burnetii* and Vamp7, Vti1a or Vti1b, indicating that the recruitment of these SNAREs proteins is a bacteria-driven process that favours the CRV biogenesis, likely by facilitating the interaction with the endolysosomal compartment.**

Introduction

Coxiella burnetii is the causative agent of Q fever, an airborne infection that usually occurs by inhalation of contaminated aerosols (Maurin and Raoult, 1999). This intracellular bacterium resides and replicates in a parasitophorous vacuole that has phagolysosome-autolysosome characteristics (Howe and Mallavia, 2000; Beron *et al.*, 2002). *C. burnetii* transits across the endocytic pathway and acquires lysosomal and autophagosomal markers at the initial infection stages, including: LAMP-1 and LAMP-2 (Heinzen *et al.*, 1996; Ghigo *et al.*, 2002), CD63, Rab7 and LC3 (Beron *et al.*, 2002; Ghigo *et al.*, 2002) among others. Once formed, the *Coxiella* replicative vacuole (CRV) displays strong fusogenic properties that lead to interaction with vesicles of the endolysosomal pathway such as endosomes and lysosomes and also with vacuoles containing inert particles such as zymosan, latex beads and heat-killed yeast (Veras *et al.*, 1994). It has also been described that vacuoles harbouring other intracellular pathogens like *Mycobacterium avium* (de Chastellier *et al.*, 1999), *M. tuberculosis* (Gomes *et al.*, 1999) and *Leishmania amazonensis* (Veras *et al.*, 1995) fuse with CRVs. In contrast, some intracellular microorganisms which evade the endocytic pathway (*Chlamydia trachomatis* or *Toxoplasma gondii*) do not interact with the large *Coxiella* parasitophorous vacuole (Heinzen *et al.*, 1996; Sinai *et al.*, 2000).

Soluble *N*-ethylmaleimide-sensitive factor attachment protein receptors (SNARE) are a superfamily of small proteins that have a domain structure with a characteristic SNARE motif (Hong, 2005; Jahn and Scheller, 2006). These proteins are major players in the final stage of docking and subsequent fusion of diverse vesicle-mediated transport events (Hong, 2005). Different sets of SNAREs are present in the two opposing membranes which then associate into complexes that are subsequently disassembled by NSF (*N*-ethyl-maleimide-sensitive fusion protein) (reviewed by Fasshauer, 2003; Hong, 2005). Initially, SNAREs were classified into two main groups, considering the 'donor' compartment and the 'acceptor' compartment, which led to their functional classification as v-SNAREs (vesicle-membrane SNAREs) or t-SNAREs (target-membrane SNAREs) (Sollner *et al.*, 1993). However, this terminology is not useful for describing homotypic fusion events, and there are also certain SNAREs which function in several transport steps with

varying partners. Therefore, SNAREs are now structurally classified into Q-SNAREs (having a Gln/Q residue) and R-SNAREs (having an Arg/R residue). On the basis of sequence homology and domain structure, the known mammalian SNAREs have been categorized as members of the syntaxin (Bennett *et al.*, 1992), Vamp (vesicle-associated membrane protein) (Baumert *et al.*, 1989) and SNAP-25 (25 kDa synaptosome-associated protein) families (Oyler *et al.*, 1989).

In the present study, we have investigated the interaction of v-SNARE members of endocytic pathway (Vamp7, Vamp8 and Vamp3) and *C. burnetii* phagosomes at early infection times. In addition, we have also analysed the presence of these SNAREs in mature CRVs. By using a Vamp7 truncated mutant and small interfering RNA (siRNA) our results indicate that this v-SNARE is involved in the development of the *Coxiella* vacuole.

Results

v-SNAREs from the endocytic pathway interact with the C. burnetii-*containing compartment at different infection times*

It has been previously reported that *C. burnetii*, once internalized, transits the endocytic pathway and finally fuses with lysosomes to generate an acidic and replicative niche with phagolysosomal characteristics (Howe *et al.*, 2010). Considering the high fusogenic characteristics of *C. burnetii* phagosomes, our aim was to investigate the possible participation of SNARE proteins from the endocytic pathway in the generation and maturation of *C. burnetii*-containing vacuoles. For this purpose, we started by determining the presence of different v-SNAREs involved in distinct steps of the endocytic pathway, such as Vamp7, which is involved in the heterotypic fusion of late endosomes and lysosomes (Pryor *et al.*, 2004); Vamp8, involved in the homotypic fusion between late endosomes (Advani *et al.*, 1999; Antonin *et al.*, 2002) and Vamp3, which regulates the recycling of plasma membrane receptors, including Tfn-R and Glut-4 and which is also enriched in recycling endosomes (Galli *et al.*, 1994; Polgar *et al.*, 2002). We analysed which of these SNAREs interacts with *Coxiella* phagosomes at early infection times and which ones are present at the CRV membrane once the large vacuole is generated. In order to evaluate these points, HeLa cells were transfected with pEGFP-Vamp8, pEGFP-Vamp7 or pEGFP-Vamp3. After 24 h of transfection, cells were infected for different periods of time (i.e. 1 h, 6 h, 12 h, 24 h and 48 h). After infection the cells were fixed and subjected to indirect immunofluorescence using specific antibodies against *C. burnetii*. The samples were analysed by confocal microscopy. Figure 1 shows confocal images of the

kinetic analysis for the different SNAREs analysed (Fig. 1A, C and E and Supplementary Fig. S1). The population of *Coxiella* phagosomes that colocalized with the tested SNAREs during the course of infection was quantified (Fig. 1B, D and F). At early infection times (i.e. 1 h), 52% ± 14% of internalized *Coxiella* colocalized with EGFP-Vamp7 (Fig. 1B) and 66.2% ± 2.8% colocalized with EGFP-Vamp8 (Fig. 1D). Similar colocalization percentages were observed at 6 h and 12 h post infection for each of these SNAREs. In contrast, a significant decrease in colocalization between *C. burnetii* and EGFP-Vamp8 was observed at 24 h of infection (21.5% ± 2.6%), and this proportion was maintained even at 48 h of infection (21.2% ± 0.2%) (Fig. 1D). The colocalization between *Coxiella* and EGFP-Vamp7 increased at 24 h of infection (59.2% ± 7.28%) and the proportion kept increasing at 48 h (70.8% ± 7.3%) (Fig. 1B). On the other hand, the colocalization between *Coxiella* and EGFP-Vamp3 was relatively constant along the course of infection; approximately 40–50% of colocalization was observed at all infection times analysed (Fig. 1F).

These results suggest that Vamp7 and Vamp3 interact with *C. burnetii* at different stages of vacuole development and persist along the infection process. In contrast, Vamp8 colocalizes with *C. burnetii* phagosomes during the first steps of the infection process (until 24 h), but the presence of this protein decreases at later infection times, when the vacuoles are fully developed.

Vamp7 partners colocalize with the C. burnetii *vacuoles*

Based on the above results indicating that Vamp7 has a strong and persistent colocalization with CRVs, we next determined the presence of some Vamp7 partners (t-SNAREs) on the *Coxiella* vacuoles. It has been previously described that Vamp7 participates in the fusion machinery of two different pathways. The better described one is the endocytic pathway, where Vamp7 plays a critical role in the heterotypic fusion between late endosomes and lysosomes in association with Syntaxin7, Syntaxin8 and Vti1b (Pryor *et al.*, 2004). As has also been described, Vamp7 participates in a non-canonical secretory pathway in association with a different repertory of t-SNAREs, which includes rBet1, Syntaxin5 and Vti1a (Siddiqi *et al.*, 2006; Flowerdew and Burgoyne, 2009). Based on this evidence, we decided to determine the presence of some of these t-SNAREs on *Coxiella* phagosomes at different infection times. For this purpose, HeLa cells were infected with *C. burnetii* and fixed at 1 h and 48 h of infection. After fixation, the cells were subjected to a double immunofluorescence using specific antibodies against *C. burnetii* and Vamp7, Vti1a or Vti1b. As shown in the confocal images (Fig. 2A), a clear colocalization between *C. burnetii* and Vamp7, Vti1a or Vti1b was
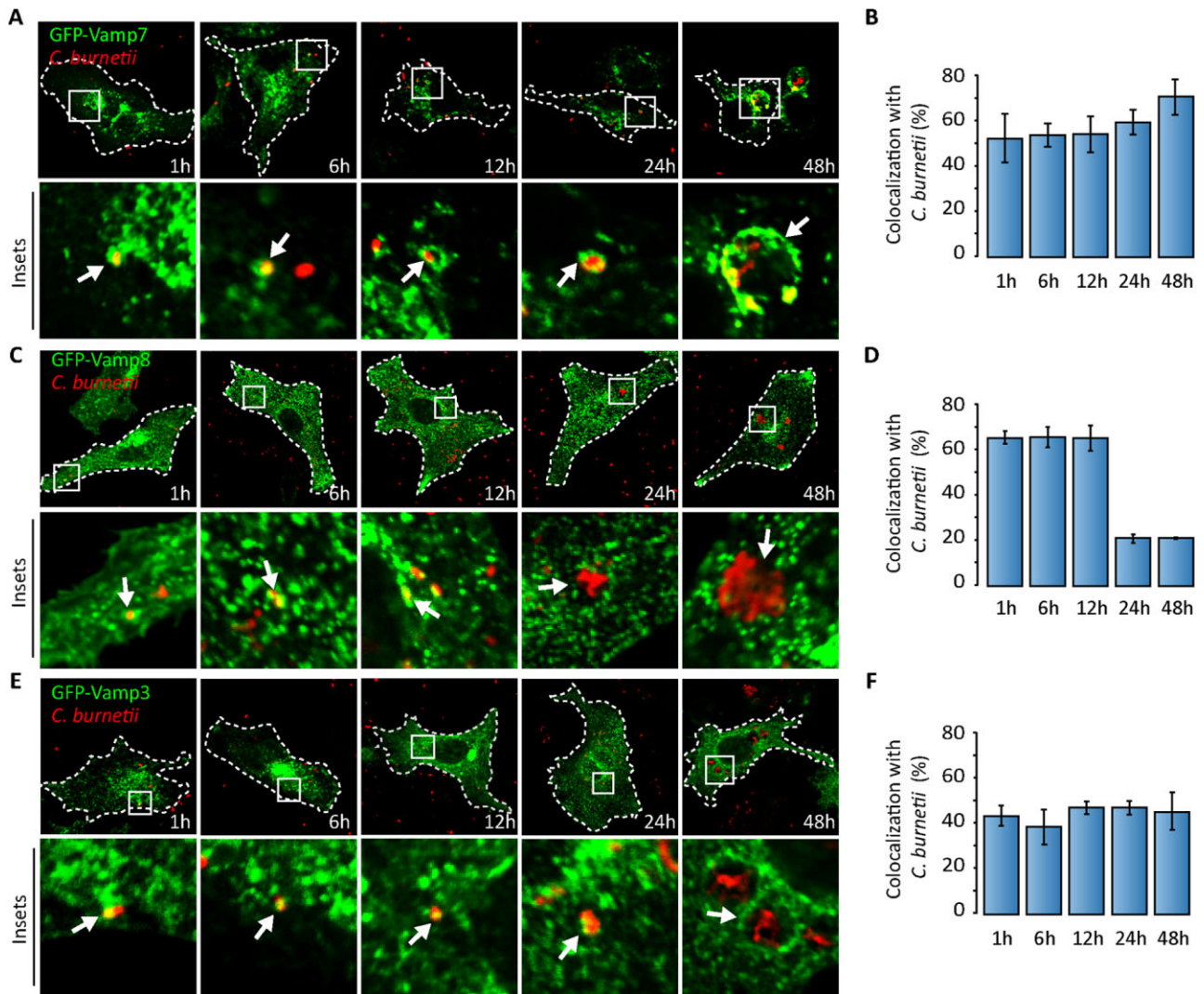
Fig. 1. Presence of v-SNARE proteins in *Coxiella* phagosomes at different infection times. Transiently transfected HeLa cells overexpressing EGFP-Vamp7 wt, EGFP-Vamp3 wt or EGFP-Vamp8 wt were infected with *Coxiella burnetii*. The cells were fixed at different infection times (1 h, 6 h, 12 h, 24 h and 48 h), subjected to indirect immunofluorescence using an antibody against *C. burnetii* (red) and visualized by confocal microscopy.
A. The images show a typical vesicular distribution of Vamp7 in the perinuclear region (green). Colocalization of EGFP-Vamp7 wt with CRVs was observed at all the infection times analysed.
B. Quantification of the experiment described in (A).
C. Images obtained by confocal microscopy showing the colocalization between EGFP-Vamp8 and CRVs at different infection times.
D. Quantification of the experiment described in (C). The bar graph shows a high colocalization at early infection times and a significant decrease at later infection times.
E. Confocal images showing the colocalization between EGFP-Vamp3 and the CRVs at different infection times. Note the patchy pattern around the vacuoles membrane at later times.
F. Quantification of the experiment described in (E), showing a similar percentage of colocalization at the distinct infection times.
Data represent the mean ± SEM of at least three independent experiments.

observed at early infection times (i.e. 1 h). However, quantification of this assay showed that the percentage of colocalization of *C. burnetii* with Vamp7 or Vti1b (60.9% ± 5% and 61.5% ± 6.6% respectively) was much higher than the colocalization with Vti1a (around 29.3% ± 6%) (Fig. 2B). At later infection times the fully developed CRVs were strongly decorated with Vamp7 and Vti1b (Fig. 2C, see arrows). In contrast, the presence of Vti1a was sparser and it presented a patchy pattern at the vacuole membrane. Quantification of these assays shows that a large amount of the vacuole population is decorated with Vti1b and Vamp7 (76.8 ± 4.4% and 74.4% ± 4.5%), whereas Vti1a was only detected in a minor fraction of the vacuoles (around 36.5% ± 0.8%), in consistency with the idea that *Coxiella* phagosomes interact mainly with the endocytic pathway.

In addition, we also assessed the presence of the endogenous t-SNARE Syntaxin-1 (Bennett *et al.*, 1993; Walch-Solimena *et al.*, 1995) at different times of infection. HeLa cells were infected for different periods of time (i.e. 1 h–48 h). After infection the cells were fixed and subjected to indirect immunofluorescence using specific antibodies against Sintaxin-1 and against *C. burnetii*. The samples were analysed by confocal microscopy. Supplementary Fig. S1 shows no colocalization between endogenous Syntaxin-1 and the *C. burnetii* phagosomes or CRV membrane at the infection times analysed.

It has been previously described that Vamp7, in association with SNAP-23 and Syntaxin4, both components of a SNARE complex, is involved in the Ca^{2+}-triggered exocytosis of conventional lysosomes (Galli *et al.*, 1998). In this process participates also Synaptotagmin VII, which is described as a Ca^{2+} sensor for membrane fusion (Martinez *et al.*, 2000). Pull-down assays have demonstrated the interaction between Vamp7 and Synaptotagmin VII (C2A domain) (Rao *et al.*, 2004). Based on the mentioned evidences indicating an interaction between these proteins, we assessed the presence of Synaptotagmin VII in *C. burnetii* vacuoles. For this purpose, HeLa cells were transfected with a plasmid encoding EGFP-Synaptotagmin VII. After 24 h of transfection the cells were infected, fixed at different infection times and subsequently subjected to indirect immunofluorescence using specific antibodies against *C. burnetii*. We observed a strong interaction between *C. burnetii* and Synaptotagmin VII at the infection times studied. Figure 2E shows the colocalization between *C. burnetii* phagosomes and Synaptotagmin VII at early infection times (1 h, 6 h 12 h) and the interaction between this protein and the CRVs at later infection times (24 h and 48 h). Quantification of this assay shows that a large amount of the *Coxiella* phagosomes colocalize with Synaptotagmin VII (Fig. 2F).

These results highlight the interaction of *C. burnetii* and the endogenous Vamp7 and its partners (t-SNAREs). Vti1b displayed a high percentage of colocalization with *Coxiella* phagosomes at 1 h of infection (comparable with the endogenous Vamp7 levels) and also maintained its presence at the latest infection time (48 h). But the results also showed a clear presence of Synaptotagmin VII in *C. burnetii* phagosomes at early infection times and a strong presence in the CRVs at 24 h and 48 h of infection.

Vamp7 recruitment is actively modulated by C. burnetii

Focused on the clear interaction between the *Coxiella* vacuole and Vamp7, the next point was to evaluate whether the arrival of Vamp7 to the vacuole is an active process modulated by the bacteria or a consequence of the normal trafficking across the endocytic pathway. *C. burnetii* has a type IV secretion system (T4SS)

(Newton and Roy, 2011) and once inside the cells, *C. burnetii* utilizes this pathogenic mechanism to inject a different repertory of bacterial effectors into the host cell cytosol in order to favour CRV development (Zamboni *et al.*, 2003; Zusman *et al.*, 2003). It has been previously described that the T4SS function can be inhibited by chloramphenicol treatment. In order to check if the association between *Coxiella* and Vamp7 is an active phenomenon that depends on bacterial protein synthesis, *C. burnetii* was pretreated with 100 μg ml^{-1} chloramphenicol for 1 h and HeLa cells were then infected, keeping the antibiotic in the culture medium. After different infection times cells were fixed and subjected to a double immunofluorescence, using specific antibodies against *C. burnetii* and Vamp7. The samples were analysed by confocal microscopy. The percentage of colocalization between *Coxiella* and Vamp7 was determined at different infection times (1 h, 6 h, 12 h and 24 h) in both antibiotic-treated and untreated cells. The quantification shows a significant difference between both conditions at all tested times (Fig. 3A). Consistently with the results presented above, we observed in the control condition a colocalization of around 55–60%, whereas with the chloramphenicol-treated bacteria the percentage of colocalization was significant smaller (around 30–35%). We also tested the colocalization of the t-SNAREs partners of Vamp7 (Vti1a and Vti1b) with *C. burnetii* under chloramphenicol treatment. In concordance with the observations for Vamp7, the antibiotic treatment caused a decrease of colocalization of both t-SNAREs (Vti1a and Vti1b) with *C. burnetii* at the different infection times studied (Supplementary Fig. S2).

Considering the active recruitment of Vamp7, the next point was to determine if the infection process affects the expression levels of endogenous Vamp7. In order to assess this point, HeLa cells were infected with *C. burnetii*. After 48 h of infection, the cells were lysed and analysed by Western blot using a specific antibody against Vamp7 (Fig. 3B). No significant differences between infected cells and the control condition were observed when this experiment was quantified (Fig. 3C).

These results clearly show that the high degree of association between *C. burnetii* and Vamp7 is an active process which depends on bacterial protein synthesis. However, the expression levels of the endogenous Vamp7 were not affected by the infection, suggesting that the high degree of colocalization of Vamp7 on the CRV is not due to upregulation of the protein.

The activity of Vamp7 is involved in optimal CRV development and Coxiella *growth*

Based on the evidence that Vamp7 is actively recruited to the vacuole membrane, we next assessed if Vamp7 is
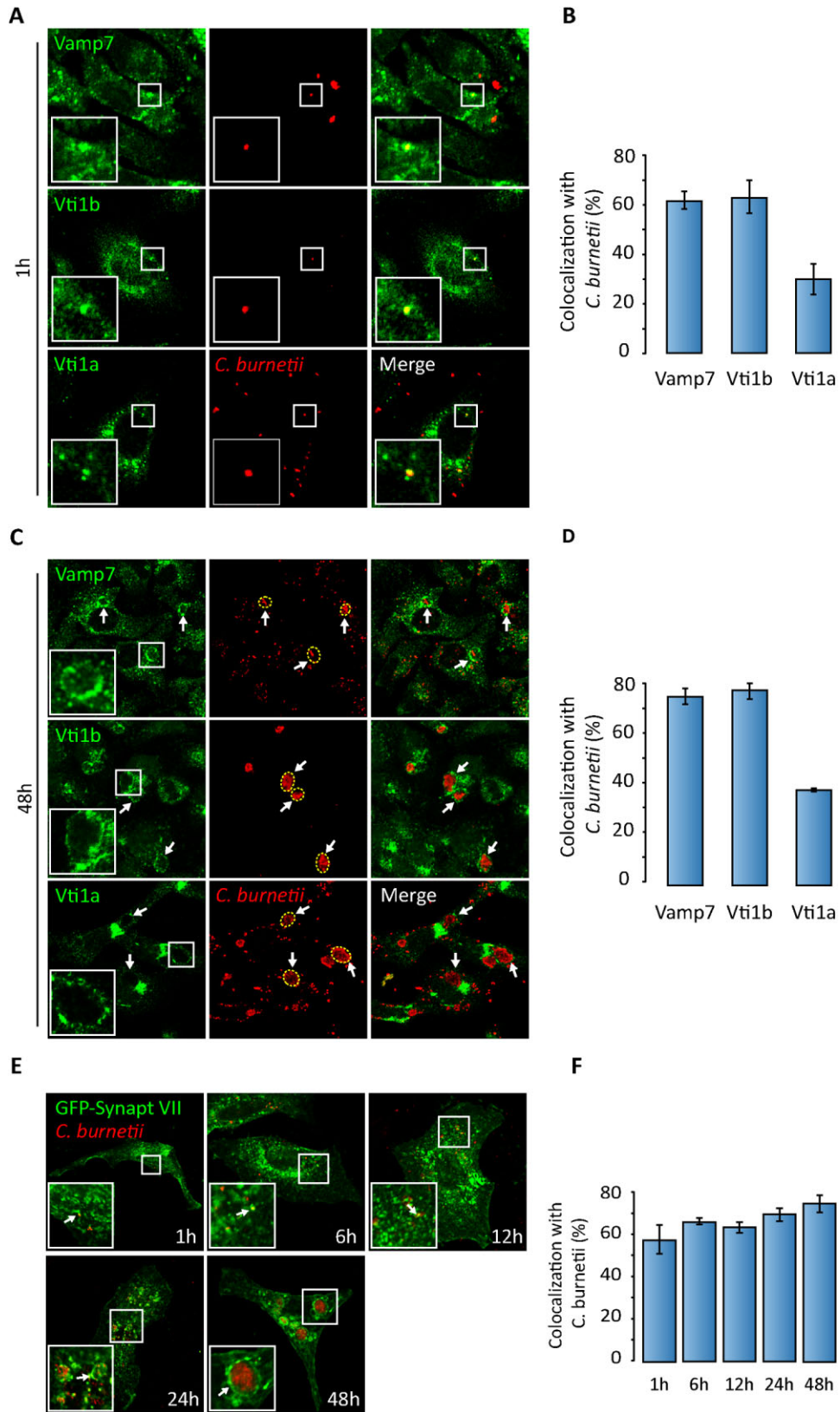
Fig. 2. t-SNAREs partners of Vamp7 as well as endogenous Vamp7 are present in *Coxiella* phagosomes at different infection times. HeLa cells were infected with *Coxiella burnetii*. After infection, the cells were fixed at different times (1 h and 48 h) and subjected to a double immunofluorescence using specific antibodies against *C. burnetii* (red) and Vti1a, Vti1b or Vamp7 (green). Afterwards, the cells were visualized by confocal microscopy.
A. The upper and middle panels show the colocalization between *Coxiella* phagosomes (red) and the t-SNAREs Vti1a and Vti1b respectively (green) at 1 h post infection (please see inset). The colocalization between *C. burnetii* phagosomes (red) and endogenous Vamp7 (green) at 1 h of infection is depicted in the lower panels.
B. Quantification of the experiment described in (A).
C. The figure shows the scarce presence of Vti1a in the vacuole membrane (showing a patchy pattern) (upper panel) (yellow dashed lines) at 48 h post infection. In contrast, the clear presence of Vti1b surrounding the CRVs is observed in the middle panel, while the detection of endogenous Vamp7 is depicted in the lower panel.
D. Quantification of experiment described in (C).
E. Transiently transfected HeLa cells overexpressing EGFP-Synaptotagmin VII were infected with *Coxiella burnetii*. The cells were fixed at different infection times (1 h, 6 h, 12 h, 24 h and 48 h), subjected to indirect immunofluorescence using an antibody against *C. burnetii* (red), and visualized by confocal microscopy. The images show a typical distribution of Synaptotagmin VII (green). Colocalization of EGFP-Synaptotagmin VII with the CRV was observed at the different infection times tested. Data represent the mean ± SEM of at least three independent experiments.
F. Quantification of the experiment described in (E).

required for the development of *Coxiella* vacuoles. In order to evaluate this point, we used a truncated mutant form of Vamp7. This truncated protein, called Vamp7 NT, contains only the amino-terminus region of Vamp7. It has been shown that when this mutant protein is overexpressed, Vamp7 activity is inhibited by competing with the endogenous protein (Martinez-Arca *et al.*, 2003). It is important to consider that prolonged overexpression of pEGFP-Vamp7 NT has a toxic effect in transfected cells. Therefore, in order to analyse the effect of this mutant in the development of the CRV we designed two different approaches. First, we decided to evaluate the biogenesis of the vacuole. For this purpose, HeLa cells were transfected with pEGFP-Vamp7 NT or pEGFP-Vamp7 wt. After the transfection period, cells were infected with *C. burnetii* with a moi of 20. After 24 h of infection, cells were fixed and subjected to immunofluorescence using an anti-*Coxiella*-specific antibody. The cells were observed by confocal microscopy (see the experimental procedure described in Fig. 4C). Interestingly, vacuole size in cells overexpressing the Vamp7 truncated mutant (EGFP-Vamp7 NT) was smaller than the vacuoles developed in cells overexpressing the wild-type form (EGFP-Vamp7 wt) (Fig. 4A), revealed by a decrease in the population of vacuoles larger than 10 μm (Fig. 4B). Due to the toxic effects of Vamp7 NT on the host cells, the second approach consisted in infecting the cells 24 h before the transfection. The purpose of this approach was to check the effect of the overexpression of the Vamp7 mutant in the growth of the *Coxiella* vacuole up to 48 h. For this, HeLa cells were infected with *C. burnetii* (moi = 10). After 24 h of infection the cells were transfected with pEGFP-Vamp7 NT or pEGFP-Vamp7 wt for another 24 h and subsequently fixed. The cells were subjected to indirect immunofluorescence to detect *C. burnetii* and visualized by confocal microscopy (see
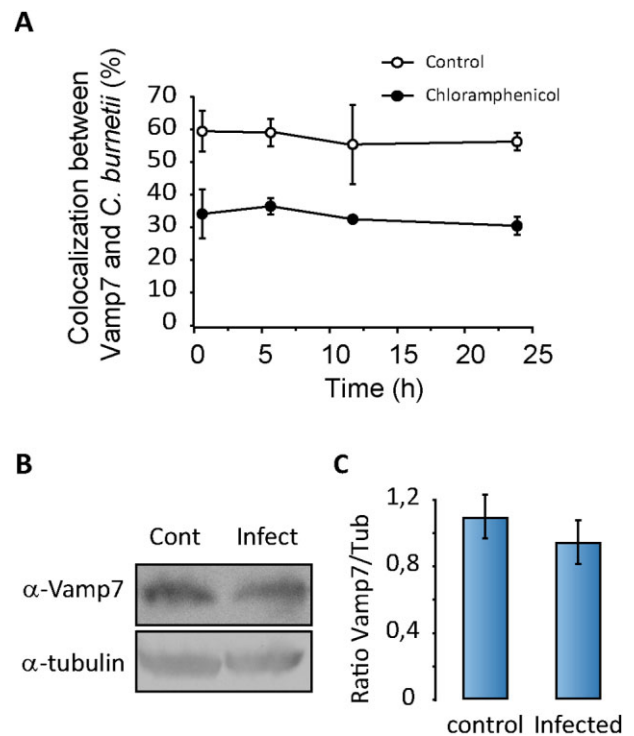

Fig. 3. Vamp7 is recruited to the *Coxiella* phagosomes in a bacterial-dependent manner. *Coxiella burnetii* was pretreated with 100 μg ml⁻¹ chloramphenicol for 30 min. HeLa cells were infected with either control or pretreated *Coxiella*, maintaining the antibiotic in the culture medium and fixed at different infection times (1 h, 6 h, 12 h and 24 h). After fixation the cells were subjected to a double immunofluorescence using specific antibodies against *C. burnetii* and Vamp7.
A. The line graph shows that in cells treated with chloramphenicol the colocalization between endogenous Vamp7 and *Coxiella* decreased significantly at all times analysed.
B. HeLa cells were infected with *C. burnetii* and after 48 h the cells were lysed and subjected to Western blot analysis.
C. Quantification of intensity of the Vamp7 bands relative to tubulin. Data represent two independent experiments.
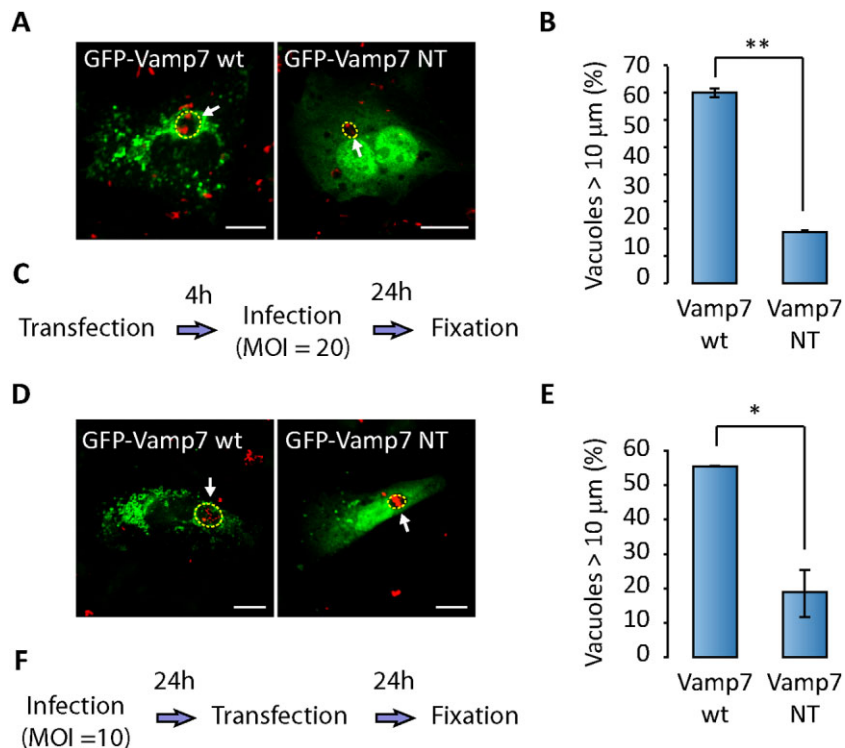
Fig. 4. The overexpression of EGFP-Vamp7 mutant (EGFP-Vamp7 NT) hampers the development of the *Coxiella* vacuole.
A. HeLa cells were transfected with pEGFP-Vamp7 NT (amino-terminal region of Vamp7) or pEGFP-Vamp7 wt. After 4 h of transfection the cells were infected with *C. burnetii* for 24 h using a moi of 20, fixed and subjected to indirect immunofluorescence using specific antibodies against *C. burnetii*. Afterwards, the cells were analysed by confocal microscopy (yellow dashed lines indicate the vacuole periphery).
B. Quantification of the vacuole diameter in cells overexpressing EGFP-Vamp7 NT compared with cell overexpressing EGFP-Vamp7 wt.
**$P \leq 0.01$.
C. Outline of the experimental procedures applied in (A).
D. HeLa cells were infected for 24 h with *C. burnetii* using a moi of 10 and subsequently transfected with pEGFP-Vamp7 NT or pEGFP-Vamp7 wt. At 48 h of infection cells were fixed and subjected to indirect immunofluorescence to detect *Coxiella* using specific antibodies (yellow dashed lines indicate the vacuole periphery).
E. Quantification of the vacuole diameter in cells overexpressing EGFP-Vamp7 NT compared with cells expressing EGFP-Vamp7 wt.
*$P \leq 0.05$.
F. Outline of the experimental procedures applied in (D).
Data represents three independent experiments.

experimental procedure described in Fig. 4F). As in the first approach, in cells overexpressing the Vamp7 mutant a notable decrease in vacuole size was observed compared with the overexpression of the wild-type protein (Fig. 4D). Quantification of this assay showed a significant reduction in the percentage of the larger vacuole population (i.e. vesicles larger than 10 μm) in cells overexpressing the Vamp7-NT mutant (Fig. 4E). It is important to take into account that overexpression of EGFP-Vamp7 wt or EGFP-Vamp7 NT did not affect *Coxiella* internalization (Supplementary Fig. S3).

In order to corroborate the requirement of a functional Vamp7 in the development of the CRV, a knock-down assay was performed. We designed a double hit protocol in order to ensure the silencing of Vamp7. For this, HeLa cells were plated in six-well plates with a small coverslip in each well. The cells were co-transfected with GFP and a siRNA against Vamp7 or a siRNA control (for more details please see *Experimental procedures*). After 48 h, the cells were transfected for a second time and after transfection, cells were infected. After 48 h the cells grown in the coverslips were fixed and subjected to a double immunofluorescence against *C. burnetii* and Vamp7. The remaining cells present in the six-well plates were scrapped and the samples were prepared for Western blot analysis. Figure 5A shows the knock-down effect in cells overexpressing GFP (lower panels). In contrast to the normal pattern of Vamp7 depicted in cells overexpressing GFP and the control siRNA (Fig. 5 upper panels, see inset), the Vamp7 label (red) was absent in cells co-transfected with the GFP vector and the Vamp7 siRNA (Fig. 5, lower panel, see inset). The Western blot assay showed the silencing of Vamp7 by the siRNA treatment relative to control siRNA (Fig. 5B). Thus, Vamp7
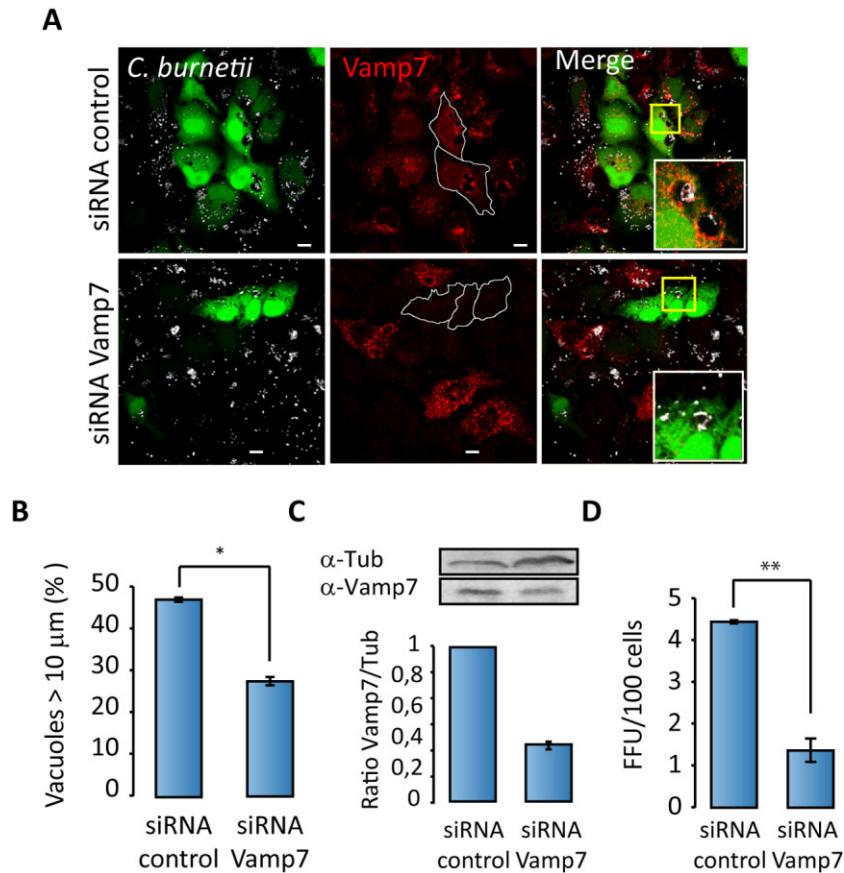
Fig. 5. The knock-down of Vamp7 impairs the full development of the *Coxiella* vacuole.
A. HeLa cells were co-transfected with pEGFP and siRNA against Vamp7 or an irrelevant siRNA as negative control. After 48 h, cells were transfected for a second time, infected with *C. burnetii* and cultured for an additional 72 h period to allow the development of the large *Coxiella* vacuole. Subsequently, cells were fixed and subjected to indirect immunofluorescence for the detection of both Vamp7 and *Coxiella* using specific antibodies. Images were captured by confocal microscopy. The panels show that in cells treated with siRNA there is an absence of Vamp7 labelling in cells expressing EGFP, indicating that Vamp7 was effectively depleted. Furthermore, the size of the *Coxiella* vacuoles decreased markedly in cells treated with siRNA against Vamp7 (inset).
B. Quantification of the vacuole diameter in cells depleted for Vamp7 compared with the control condition. Data represent the mean $\pm$ SEM of at least three independent experiments in which at least 200 vacuoles were scored in each experiment (*$P \leq 0.01$).
C. Western blot of the assay described in (B) and quantification of intensity of the Vamp7 bands relative to tubulin. Data represent two independent experiments.
D. HeLa cells were co-transfected with pEGFP and a siRNA against Vamp7 or an irrelevant siRNA as negative control. After 24 h, cells were infected with *C. burnetii* and following 24 h of infection the cells were transfected for a second time, and cultured for an additional 24 h period to allow the development of the large *Coxiella* vacuole. The cells were then lysed by sonication and the supernatant was diluted (1:500) and used to infect Vero cells. After 72 h of incubation (chase), cells were fixed and examined by fluorescence microscopy. Data represent the mean $\pm$ SEM of at least two independent experiments where at least 1000 cells were scored in each experiment (**$P \leq 0.01$).

silencing caused a decrease in the CRVs size, revealed by a significant reduction in the larger (10 μm) vacuole population (Fig. 5C).

To asses the effect of knocking down Vamp7 in bacteria replication, a focus-forming unit (FFU) assay was designed. For this, HeLa cells were co-transfected with pEGFP and an irrelevant siRNA or a siRNA against Vamp7. After 24 h, cells were infected with *C. burnetii* and following 24 h of infection the cells were transfected for a second time. At 48 h of infection, cells were scraped and lysed by sonication. Sonicates were diluted in infection Dulbecco's modified Eagle's medium (D-

MEM) and a monolayer of Vero cells were infected with a dilution of the supernatant obtained (1:500). After 72 h of incubation (chase), cells were fixed and examined by fluorescence microscopy (please see *Experimental procedures* for more details). The FFU assay showed a significant decrease in the replicative capacity of *C. burnetii* in cells subjected to Vamp7 knock-down, indicating an active role of this protein in *Coxiella* growth (Fig. 5D).

Taken together, these results suggest that Vamp7 has an important role in both bacteria replication and optimal CRVs development, evidenced by a reduction in vacuole
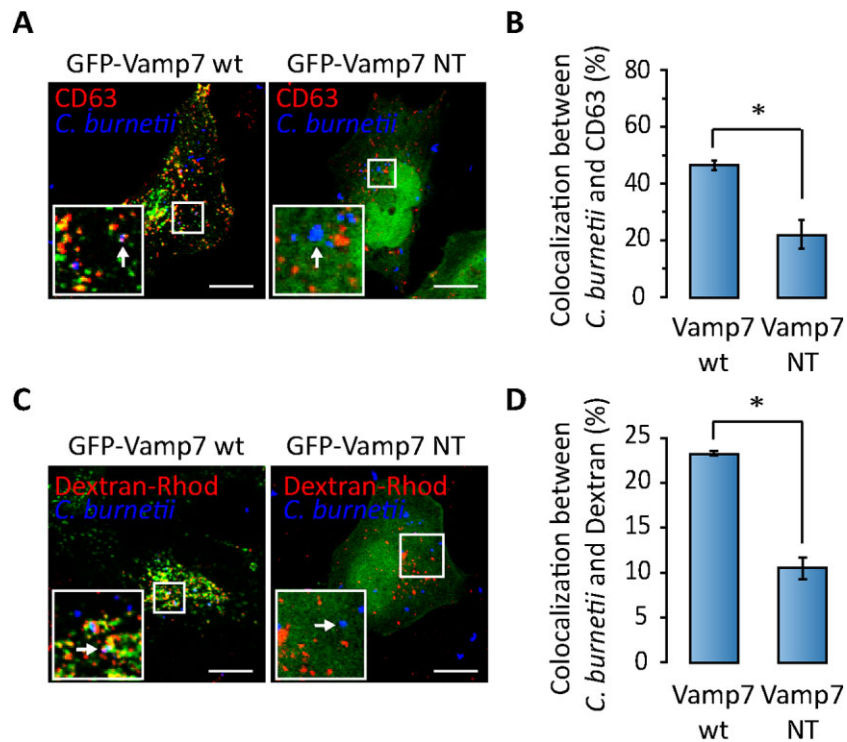
Fig. 6. Overexpression of the truncated mutant of Vamp7 NT alters the heterotypic fusion of the *C. burnetii* vacuoles.
A. HeLa cells transiently transfected with EGFP-Vamp7 wt or EGFP-Vamp7 NT were infected with *Coxiella burnetii*. At 2 h of infection, cells were fixed and subjected to a double immunofluorescence using specific antibodies against CD63 (LAMP 3) and *C. burnetii*. The cells were analysed by confocal microscopy.
B. Quantification of the colocalization between *C. burnetii* and CD63 shows a decrease in the percentage of colocalization in cells overexpressing the truncated mutant (EGFP-Vamp7 NT).
C. HeLa cells transiently overexpressing EGFP, EGFP-Vamp7 wt or EGFP-Vamp7 NT were incubated for 2 h with 5 μg ml^{-1} dextran-rhodamine in order to label lysosomes. The left panels show that in HeLa cells overexpressing EGFP-Vamp7 wt the *Coxiella* phagosomes (blue) colocalize with dextran-rhodamine vesicles (red), whereas a decreased colocalization is observed in cells overexpressing EGFP-Vamp7 NT (right panels), suggesting that the fusogenic capacity with the endocytic pathway was altered. Bars: 20 μm.
D. Quantification of the percentage of colocalization of *C. burnetii* and dextran-rhodamine. Fifty cells were counted in each condition.
Data represent the mean ± SEM of at least three independent experiments (*$P \leq 0.05$).

size when the function of Vamp7 was affected either by the overexpression of the Vamp7 truncated mutant or by Vamp7 silencing.

Overexpression of the mutant Vamp7 NT alters the heterotypic and homotypic fusion capacity of the CRVs

As mentioned in the introduction, Vamp7 is involved in the heterotypic fusion between late endosomes and lysosomes (Pryor *et al.*, 2004); since the CRV presents phagolysosomal characteristics, the next question was: is Vamp7 required for the heterotypic fusion between the CRVs and the endocytic compartments? To answer this question we decided to detect CD63, a transmembrane protein also called LAMP-3 (lysosomal associated membrane protein 3) present in vesicles of the late endocytic pathway. To corroborate the participation of Vamp7 in the heterotypic fusion of the *C. burnetii* vacuoles, HeLa cells were transfected with pEGFP-Vamp7 wt or the truncated mutant pEGFP-Vamp7 NT. After 24 h of transfection the

cells were infected with *C. burnetii* for 2 h, fixed and subjected to a double indirect immunofluorescence against *C. burnetii* and CD63. The samples were analysed by confocal microscopy. Figure 6A shows transfected cells overexpressing EGFP-Vamp7 wt or EGFP-Vamp7 NT where the colocalization between *Coxiella* (blue) and CD63 (red) is observed. Quantification of this assay indicated that in cells transfected with EGFP-Vamp7 NT the percentage of colocalization between CD63 and *Coxiella* was significant smaller (22.5% ± 6.3%) than in cells overexpressing EGFP-Vamp7 wt (47.5% ± 2.1%) (Fig. 6B). In order to assess whether the fusion of CRVs with lysosomes was also affected, we utilized a different approach. It has been previously demonstrated that molecules internalized by fluid phase endocytosis can be found in vacuoles containing *C. burnetii*. To analyse the fusion capacity of the *Coxiella* phagosomes, specifically with lysosomes, HeLa cells were incubated with 5 μg ml^{-1} dextran-rhodamine for 2 h and then the cells were washed three times with PBS and transfected with pEGFP-Vamp7

wt or pEGFP-Vamp7 NT. After 24 h of transfection, cells were infected with *C. burnetii* for 2 h. Subsequently, cells were fixed and subjected to immunofluorescence using an antibody against *C. burnetii*. The Fig. 6C shows the colocalization between lysosomes labelled with dextran (red) and *C. burnetii* (blue). Interestingly, in cells over-expressing EGFP-Vamp7 NT the colocalization was significant smaller than in those overexpressing EGFP-Vamp7 wt. In cells overexpressing the Vamp7 mutant the percentage of colocalization was 10.5% ± 1.7% in contrast to the wild-type form of Vamp7, which displayed a higher percentage of colocalization of 23.3% ± 0.387% (Fig. 6D).

The enlargement of the *C. burnetii* vacuole is achieved by both heterotypic and homotypic fusion events. There-fore, the next step was to verify if Vamp7 was also involved in the homotypic fusion between *Coxiella* phago-somes. HeLa cells were plated and infected with *C. bur-netii*; after 24 h of infection cells were transfected with pEGFP-Vamp7 NT or pEGFP-Vamp7 wt. At 48 h of infec-tion cells were infected with mCherry-*Coxiella* for 5 h. Subsequently, cells were fixed and subjected to indirect immunofluorescence against *Coxiella*. Confocal images of this assay show HeLa cells overexpressing EGFP-Vamp7 wt or EGFP-Vamp7 NT with *Coxiella* vacuoles. As expected, in cells overexpressing EGFP-Vamp7 wt the mCherry-*Coxiella* was observed colocalizing in the large CRVs. In contrast, very little colocalization was observed in cells overexpressing the Vamp7 truncated mutant (Fig. 7A, see inset, arrows). Quantification of this assays showed a significant decrease in the colocalization between both mCherry-*Coxiella* and *C. burnetii* wt when the Vamp7 mutant was overexpressed (27.74% ± 6.46%), in contrast to the overexpression of the wild-type form of the protein (59.78% ± 3.17%) (Fig. 7B).

To verify the participation of Vamp7 in the homotypic fusion of the CRVs, we analysed the fusion process by time-lapse microscopy. HeLa cells were transfected with pEGFP-Vamp7 wt and after 24 h of transfection the cells were infected with *C. burnetii* (moi = 10) for additional 24 h. Afterwards, the cells were mounted into an *in vivo* camera to be analysed by confocal microscopy. Figure 7C shows a HeLa cell overexpressing EGFP-Vamp7 wt with multiples CRVs vacuoles at the initial step (0 min); the inset depicts two CRVs decorated with EGFP-Vamp7 in close proximity (Fig. 7, upper panel, delineated cell and inset). After 70 min the same cell was observed with a unique *Coxiella* vacuole as a result of the fusion event. Figure 7D shows the sequence of the total time-lapse analysed. Panel g shows that the two *Coxiella* vacuoles are in contact with each other; an enrichment of Vamp7 in the contact area could be observed (see arrow). Next, the CRVs begin to fuse and, subsequently, fusion of both vesicles was completed. Interestingly, after the fusion, a

long tubule that likely represents recycling of molecular membrane components is visualized (see arrowhead in panel n). At the end of the sequence there is a unique CRV as a result of the fusion of the two vacuoles (Movie S1). In order to demonstrate the specific require-ment of Vamp7 in the homotypic fusion of *Coxiella* vacu-oles, the same experiment was performed in cells overexpressing EGFP-Vamp8, but in this case no evident participation of this SNARE protein in the fusion process was observed (Supplementary Fig. S5 and Movie S2).

Taken together these results indicated that the overex-pression of the Vamp7 truncated mutant inhibited both the homotypic fusion between *Coxiella* phagosomes and the heterotypic fusion between *Coxiella* phagosomes and lysosomes labelled with dextran or late endocytic vesicles (CD63). In addition, the results also indicate that Vamp7 is involved in the homotypic fusion of the CRVs and that this protein is enriched at the vacuolar fusion site.

Overexpression of the tetanus toxin affects the formation and growth of the CRVs

We have shown that EGFP-Vamp3 wt colocalizes with the earlier *Coxiella* phagosomes and it is also present at the CRVs with a patchy pattern at later infection times. As mentioned, Vamp3 is a SNARE involved in the recycling of plasma membrane receptors, including Tfn-R and Glut-4 and it is also enriched in recycling endosomes (Galli *et al.*, 1994; Polgar *et al.*, 2002).

It has been described that the light chains of the tetanus toxin (TeNT) and botulinum toxins (BoNTs) have a specific proteolytic effect on certain SNARE proteins (Humeau *et al.*, 2000; Turton *et al.*, 2002; Proux-Gillardeaux *et al.*, 2005). Tetanus neurotoxin proteolytically cleaves Vamp1, Vamp2 and Vamp3 and it has been used extensively to experimentally inhibit these SNAREs in cellular studies (Gaisano *et al.*, 1994; Tayeb *et al.*, 2005; Fields *et al.*, 2007). It should be noted that Vamp3 is the only known v-SNARE sensitive to TeNT that participates in the endo-cytic pathway, while Vamp1 and Vamp2 are involved in the exocytic process. It is important to take into account that overexpression of the catalytic chain of TeNT for extended periods of time has a toxic effect similar to the overexpression of EGFP-Vamp7 NT in the host cells. Therefore, we performed two different approaches to examine the effect of TeNT in the development of the CRVs (Fig. 4A and D). To address whether TeNT overex-pression alters the vacuole biogenesis, HeLa cells were co-transfected with pEGFP-Vamp3 wt and tetanus toxin light chain (pCMV5-TeNT LC) or just with GFP-Vamp3 wt. After transfection cells were infected with *C. burnetii* (moi = 20), fixed at 24 h of infection and subsequently subjected to indirect immunofluorescence using specific antibodies against *C. burnetii*. In Fig. 8 the confocal
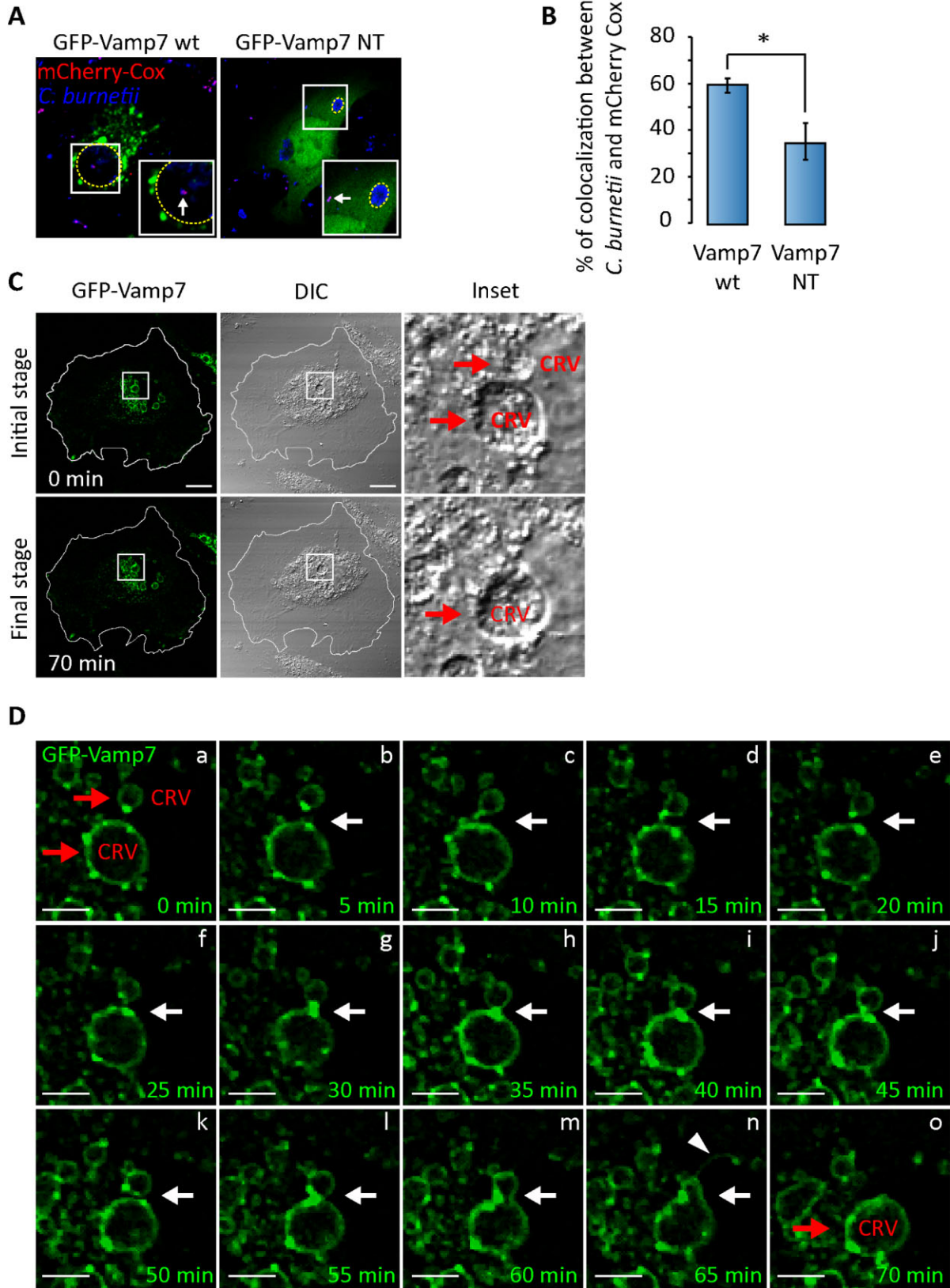
Fig. 7. The homotypic fusion between *Coxiella* containing phagosomes is altered by overexpression of the mutant EGFP-Vamp7 NT.
A. HeLa cells were infected with *Coxiella burnetii* for 24 h and transfected with pEGFP-Vamp7 wt or pEGFP-Vamp7 NT. After 24 h of transfection, cells were infected with mCherry *Coxiella* for 2 h and fixed and subjected to indirect immunofluorescence using specific antibodies against *C. burnetii* (blue). The cells were analysed by confocal microscopy. Insets show mCherry-*Coxiella* (arrows) (yellow dashed lines indicate the vacuole periphery).
B. Quantification of the colocalization between *C. burnetii* and mCherry-*Coxiella*. The bar graph shows a decrease in the percentage of colocalization under EGFP-Vamp7 NT overexpression (*$P \leq 0.05$).
C. HeLa cells transiently overexpressing EGFP-Vamp7 wt were infected with *C. burnetii* (moi = 10). After 24 h the cells were mounted into an *in vivo* camera and analysed by confocal microscopy for 70 min. Bars: 20 μm.
D. Insets of the experiment described in (C), showing the sequences of the movie (every 5 min). Red arrows indicate the CRVs; white arrows points to the fusion site. Bars: 5 μm.

---

images show a typical punctate distribution of Vamp3 under control condition (Fig. 8A, left panel). In contrast, when EGFP-Vamp3 was coexpressed at the same time with TeNT, the vesicular pattern of Vamp3 was changed to a soluble distribution due to the toxin effect. The *Coxiella* vacuoles developed under this condition, revealing a decrease in their size (Fig. 8B). Quantification of this experiment showed a significant decrease of the vacuole
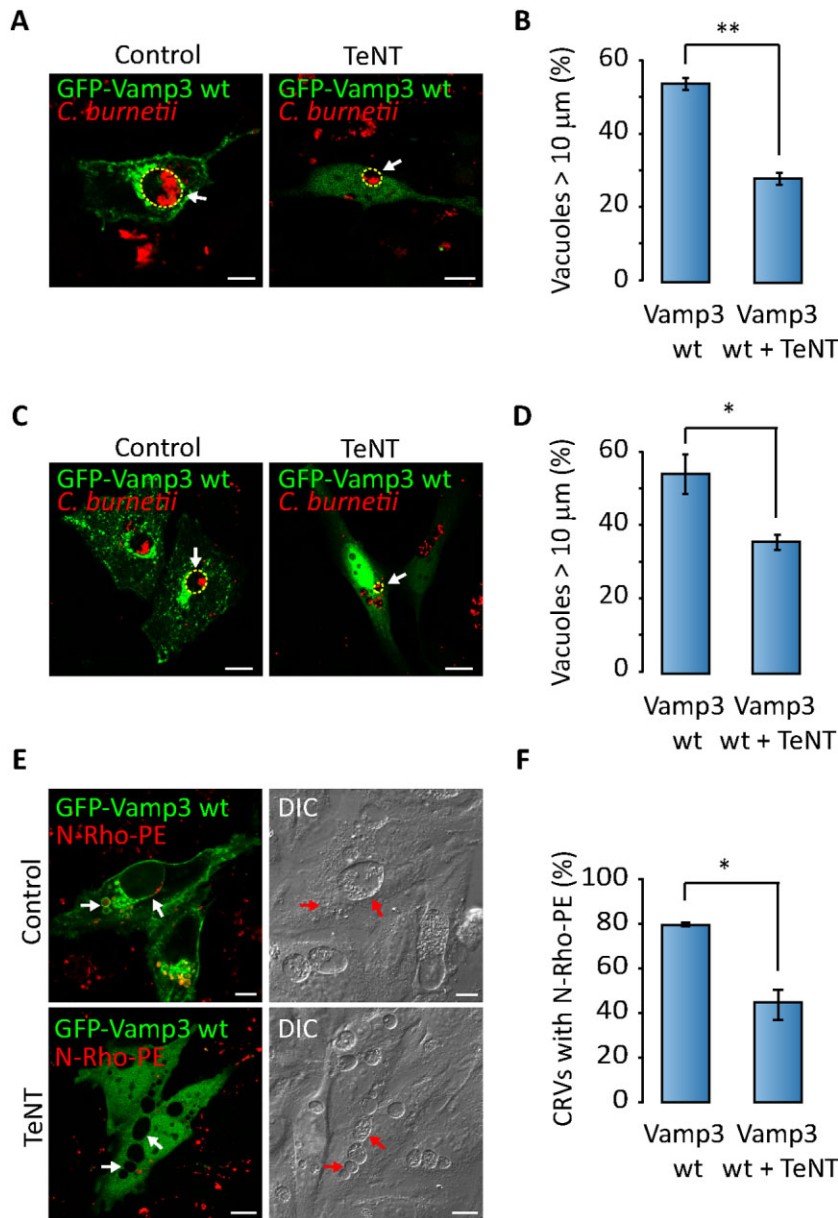

Fig. 8. Overexpression of the tetanus toxin hampers the CRVs development and the heterotypic fusion with MVB.
A. HeLa cells were co-transfected with pEGFP-Vamp3 wt and tetanus toxin light chain (pCMV5-TeNT LC) or transfected with EGFP-Vamp3 wt alone. After transfection cells were infected with *C. burnetii* (moi = 20); afterwards, the cells were fixed at 24 h of infection and subjected to indirect immunofluorescence using specific antibodies against *C. burnetii* (yellow dashed lines indicate the vacuole periphery).
B. Quantification of the experiment described in (A).
C. HeLa cells were infected with *C. burnetii* for 24 h (moi = 10). Following this period of time, the cells were co-transfected with both pCMV5-TeNT LC and pEGFP-Vamp3 wt or with pEGFP-Vamp3 wt. After 24 h, the cells were fixed and subjected to immunofluorescence against *C. burnetii* and observed by confocal microscopy (yellow dashed lines indicate the vacuole periphery).
D. Quantification of the experiment described in (C).
E. HeLa cells were co-transfected with both pEGFP-Vamp3 wt and pCMV5-TeNT LC or with pEGFP-Vamp3 wt and infected with *C. burnetii* (moi = 20). After 24 h of infection the cells were incubated 1 h at 4°C with N-Rh-PE (in order to attach the lipid to the plasma membrane). Next, the cells were washed with PBS and incubated 1 h at 37°C to induce the internalization of the lipid. After internalization the cells were washed with PBS and mounted in the *in vivo* camera and observed by confocal microscopy.
F. Quantification of the experiment described in (E).
Arrows indicate the CRVs. *$P \leq 0.05$; **$P \leq 0.01$. Bars: 10 μm.

diameter by overexpression of TeNT (EGFP-Vamp3 wt alone) (Fig. 8B).

Also, in order to analyse the enlargement of the *Coxiella* vacuole in cells transfected with the toxin, HeLa cells were first infected with *C. burnetii* for 24 h (moi = 10). After this period of time, the cells were co-transfected with both pCMV5-TeNT LC and pEGFP-Vamp3 wt or with pEGFP-Vamp3 wt. After 24 h, the cells were fixed and subjected to immunofluorescence against *C. burnetii*. Figure 8C shows confocal images of cells with smaller vacuoles under TeNT overexpression (yellow dashed lines); the quantification of this assay demonstrated a significant decrease of the vacuole diameter (Fig. 8D).

These results indicate the involvement of Vamp3 in both the *C. burnetii* vacuole biogenesis and enlargement, evidenced by the reduction in the CRVs size after the cleavage of Vamp3 of the host cell by the tetanus toxin action.

Vamp3 is involved in the fusion of CRVs and multivesicular bodies

It has been previously reported that Vamp3 is necessary for the fusion of autophagosomes and multivesicular bodies (MVBs) (Fader *et al.*, 2009). Considering the phagolysosome-autolysosomal characteristics exhibited by the large CRVs, we assessed the role of Vamp3 in the fusion between the CRVs and MVBs. For this purpose, we employed the fluorescent lipid analogue N-Rh-PE to specifically label MVBs (Vidal *et al.*, 1997). HeLa cells were transfected with pEGFP-Vamp3 wt or with both pEGFP-Vamp3 wt and pCMV5-TeNT LC and infected with *C. burnetii* (moi = 20). After 24 h of infection the cells were incubated 1 h at 4°C with N-Rh-PE (in order to attach the lipid to the plasma membrane); next, the cells were washed three times with PBS and incubated for 1 h at 37°C to induce the internalization of the lipid. After internalization the cells were washed with PBS and mounted in the *in vivo* camera and observed by confocal microscopy. Figure 8E shows CRVs decorated by EGFP-Vamp3 wt containing N-Rh-PE inside (red channel upper panels). In contrast, when the tetanus toxin was coexpressed with the wild-type form of Vamp3 no lipid label inside the CRVs was observed (Fig. 8E lower panels). Quantification of this assay showed a significant decrease of N-Rh-PE inside the vacuoles when the tetanus toxin was overexpressed in the host cells (Fig. 8F). The described results indicate that the overexpression of the tetanus toxin affected the presence of N-Rh-PE in the CRVs, which suggests that the heterotypic fusion between CRVs and MVBs was hampered by the toxin. In addition, the role of Vamp3 in heterotypic fusion between the *Coxiella* phagosomes and late endosomes/lysosomes was assessed. Quantification of the colocalization between CD63 and *Coxiella* phagosomes indicated that the overexpression of

the TeNT did not affect these heterotypic fusion (Supplementary Fig. S4A). Similar results were obtained when homotypic fusion was analysed since TeNT overexpression did not affect the fusion between *Coxiella* phagosomes (Supplementary Fig. S4B).

Discussion

The key for the survival and replication of *C. burnetii* in host cells is its capacity to develop the large phagolysosome-autolysosomal compartment where the bacterium benefits of the acidic pH for its metabolic activation, resisting its degradative function. CRV transits the endolysosomal and autophagic pathway to form a large phagolysosome with characteristics of autophagolysosomes (Beron *et al.*, 2002; Romano *et al.*, 2007). It is known that *C. burnetii* actively manipulates host processes for successful replication, likely via its Dot/Icm type IV secretion system (T4SS), since CRV requires bacterial protein synthesis for its maturation. These data are consistent with the appearance of a large and spacious vacuole at 48 h of infection in coincidence with the exponential growth of this organism that occurs at 48–96 h after infection and it is visible by confocal images of DAPI-stained Vero cells infected with *Coxiella* (Zamboni *et al.*, 2001) or by electron microscopy (Coleman *et al.*, 2004).

Vacuole development is carried out via fusion events that supply enough membrane and specific proteins of the host cell needed to enlarge and mature the *Coxiella* replicative compartment. These events involve homotypic fusion between different *Coxiella* phagosomes and heterotypic fusion with vesicles from the endocytic and the secretory pathways (i.e. lysosomes, endosomes, MVBs and secretory vesicles) in order to consolidate the replicative compartment. The presence of several Rab proteins in the CRVs has been previously described (i.e. Rab5, Rab7, Rab1). These proteins participate in the regulation of the intracellular traffic of the host cell and have an important role in the biogenesis and enlargement of the CRVs (Beron *et al.*, 2002; Colombo *et al.*, 2006; Campoy *et al.*, 2011). In the present report, we demonstrate the participation of another kind of molecules involved in intracellular trafficking, the SNARE proteins, which are key components of the fusion machinery. A subset of different SNAREs involved in the endocytic pathway, more specifically in the fusion of endosomes (or MVBs) and lysosomes, were analysed. The presence of Vamp7, Vamp8, Vamp3 and Vti1b in the CRVs indicates that the *C. burnetii* vacuoles have the machinery to fuse with those compartments.

Vamp7 has a central role in lysosomal fusion. Considering the relevant interaction between *C. burnetii* and the endocytic/degradative pathway, we focused our studies on this protein. Initially, we determined the presence of

Vamp7 all along the infection process, observing a clear colocalization with the *C. burnetii* phagosomes at early infection times and a very strong label of Vamp7 in the fully developed *Coxiella* vacuoles. We also detected the presence of t-SNAREs partners of Vamp7 in the CRVs, as well as the Vamp7-interacting protein synaptotagmin VII, indicating that others members of the SNARE complex were present at the *C. burnetii* vacuoles, likely contributing to the vesicular fusion events.

Interestingly, based in our chloramphenicol studies, we can infer that for optimal recruitment of Vamp7 to the vacuole membrane it is necessary a continuous production of *Coxiella* proteins. Consistent with this observation, different SNARE-like proteins have been identified in *Chlamydia* and *Legionella* (Delevoye *et al.*, 2004; Morozova *et al.*, 2004). IncA is a protein expressed by *Chlamydia* on the surface of the infectious vacuole. This protein displays two SNARE-like motifs and interacts directly with mammalian SNAREs (Delevoye *et al.*, 2004; 2008). In our system we have established that *C. burnetii* pretreated with chloramphenicol recruited Vamp7 at lower levels than the non-treated bacteria. Thus, it is tempting to speculate that a functional *Coxiella* secretion system is necessary to enhance the recruitment of Vamp7 to the CRVs in order to benefit the interaction with lysosomal vesicles. However, a basal colocalization between *C. burnetii* and Vamp7 was conserved under antibiotic treatment. This suggests that transit across the endocytic pathway is maintained even in the absence of a functional secretory system. Therefore, the recruitment of Vamp7 to the *Coxiella* vacuole depends, in part, on the normal endocytic transport of the host cell, but it is also actively modulated by the bacteria. Considering the strong and active recruitment of Vamp7 to the CRVs we propose that *C. burnetii* secretes factors which drive the interaction of the *Coxiella* phagosomes with the lysosomal compartment via the recruitment of Vamp7, favouring the fully development of the CRVs. In concordance with this hypothesis, we have demonstrated that both the overexpression of a Vamp7 truncated mutant and the silencing of the endogenous protein affects the normal development of the CRVs, as evidenced by a decrease of the vacuoles size. In addition, we have also determined the replication capacity of the bacteria by a FFU assay in cells subjected to Vamp7 knock-down. We observed a significant decrease in bacteria replication when Vamp7 was silenced which indicates that this SNARE protein is involved in the generation of an appropriate environment for bacteria growth. Taking into consideration the highly fusogenic capacity of the *Coxiella*-containing vacuole, which interacts with several intracellular compartments, the mentioned finding, highlights the significance of this Vamp7-mediated fusion event in *Coxiella* intracellular survival. Our present results support the model depicted

in Fig. 9 indicating that Vamp7 is a key molecular component that favours not only the formation of the large replicative niche but also the acquisition of critical factors and nutrients for bacterial growth.

As indicated above, the generation of smaller *Coxiella*-containing vacuoles is likely due to an alteration caused by the overexpression of the Vamp7 truncated mutant, which affects both the homotypic fusion among *Coxiella* phagosomes and the heterotypic fusion between the CRVs and late endocytic vesicles (CD63) and lysosomes (dextran assay). It should be noted that we have detected, by an *in vivo* experiment, the presence of Vamp7 in the fusion contact region between *Coxiella* phagosomes. An enrichment of Vamp7 was observed between the two different *Coxiella* phagosomes at the initial steps of the fusion process. During the docking process, just before the fusion, a strong enrichment of Vamp7 was observed at the vacuoles contact site. The high intensity of fluorescence in the contact region (i.e. accumulation of GFP-Vamp7) has similarities with previous evidence observed in the homotypic fusion between early endosomes, where an endosome docking reaction followed by an 'explosive' fusion event was observed in BHK cell overexpressing GFP-rab5:Q79L (Roberts *et al.*, 1999). In addition, it has been described that, after fusion of two vesicles, an asymmetric fission occurs, producing a tubule and a round-shaped vesicle (Maxfield and McGraw, 2004; Mayorga and Campoy, 2010). Curiously, the very instant that *Coxiella* phagosomes fused with each other (Movie S1), a tubular structure labelled with Vamp7 was formed (Fig. 7D panel n, arrowhead), indicating the formation of both the vesicle (CRV) and the tubule as a result of the fusion event. This tubule likely represents a means of recycling membrane components for a subsequent fusion event.

It has been previously reported that Vamp3, which allows the maturation of the autophagic vacuole, is required for the fusion between MVBs and autophagosomes (Fader *et al.*, 2009). Moreover, we have previously demonstrated that the *Coxiella* vacuoles colocalize with LC3, the typical autophagic marker (Beron *et al.*, 2002) and that LC3 is actively recruited to the vacuole membrane at different infection times (Romano *et al.*, 2007). In addition, we have shown that autophagy induction favours *C. burnetii* replication and bacterial viability (Gutierrez *et al.*, 2005; Colombo *et al.*, 2006; Romano *et al.*, 2007). Concordantly with these evidence, we observed that overexpression of the tetanus toxin (TeNT), which specifically cleaves Vamp3 in the host cells, hampered the normal development of the CRVs. Considering the high fusogenic properties of the CRVs, it is likely that multivesicular bodies interact with the *Coxiella* vacuoles. When TeNT was overexpressed in the host cells, the N-Rh-PE (specific marker of MVBs) did not colocalize with the *Coxiella*
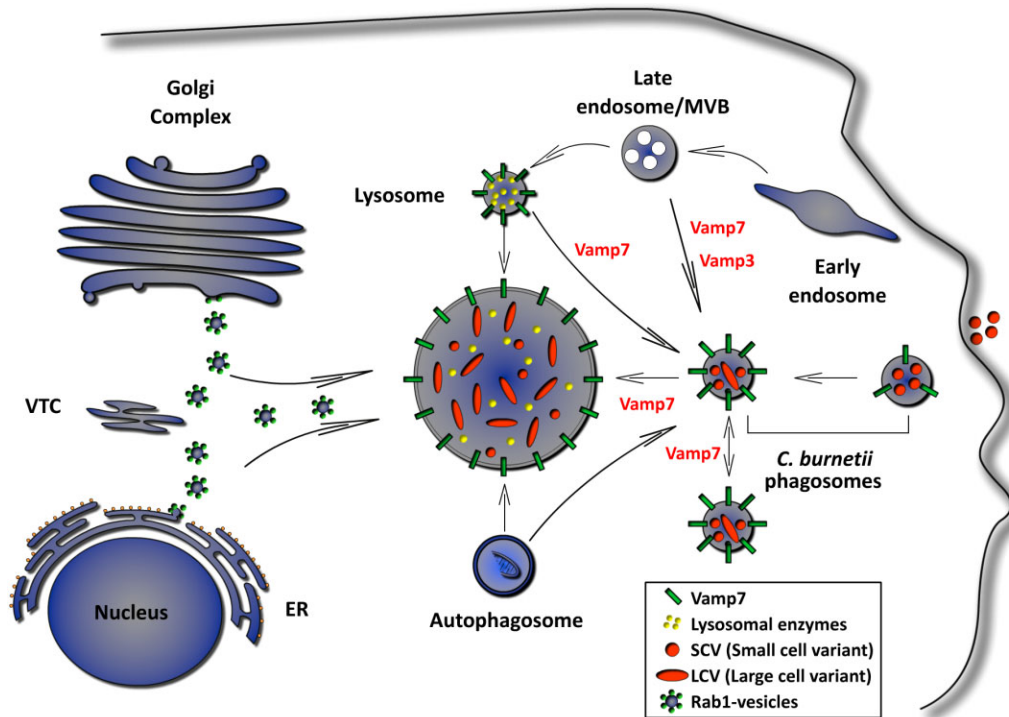
Fig. 9. Model showing the participation of Vamp7 in the *Coxiella* vacuole development. Upon internalization, bacterium phagosomes interact with the endocytic pathway (the protein Vamp7 is present at the vacuole membrane). These *Coxiella*-containing phagosomes also interact with degradative organelles such as lysosomes. These fusion events contribute to generate a proper environment for the replication process. The highly fusogenic properties of the *Coxiella* phagosomes would contribute not only to the formation of the large replicative niche but also to the acquisition of key factors and nutrients that favour the transformation of the bacteria into the replication-competent form (i.e. large cell variant).

vacuoles, indicating that fusion with multivesicular bodies was impaired.

The evidence presented in this reports indicates that SNAREs proteins of the endocytic pathway interact with *C. burnetii*-containing vacuoles. This bacterium is able to actively manipulate the recruitment of Vamp7 in order to stimulate the interaction with vesicles of the endocytic-lysosomal pathway to promote proper CRV development. Vamp7 has also a key role in the homotypic fusion which also contributes to the vacuole enlargement. There are different SNAREs that remain to be tested; for example, we have previously described that the early secretory pathway contributes to the development of the CRVs (Campoy *et al.*, 2011); therefore, it should be important to analyse SNAREs involved in this pathway. Moreover, it is tempting to speculate that *C. burnetii* would secrete factors with SNARE motif, like *Chlamydia* or *Legionella*. In fact, *C. burnetii* isolates encode numerous hypothetical proteins with predicted CCDs (coiled-coiled domains), a structure that consists of interacting heptad-helices which prevails in the SNARE proteins. Indeed, an eucaryotic-like protein of *Coxiella* isolates called Cbu0519 has been identified and this protein has a motif similar to a SNARE associated Golgi protein (Beare *et al.*, 2009). In recent years, novel genetic tools and

host cell-free growth of *C. burnetii* have been developed (Omsland *et al.*, 2009; Beare *et al.*, 2011) which will enable to generate key mutants to study fundamental aspects of the vesicular trafficking events involved in *Coxiella*-vacuole development.

Experimental procedures

Materials

Minimum essential medium alpha medium (α-MEM) and D-MEM were obtained from Gibco Laboratories (Invitrogen, Argentina); fetal bovine serum (FBS) was obtained from NATOCOR S.RL (Córdoba, Argentina). Rabbit polyclonal anti-*Coxiella* antibody and mCherry *C. burnetii* were generously provided by Dr Robert Heinzen (Rocky Mountain Laboratories, NIAID, NIH, Hamilton, MT, USA). Vamp7 and control siRNAs were obtained from BIONEER (Korea).

Cell culture

Vero cells, HeLa cells and Chinese hamster ovary cells (CHO) were grown on coverslips in D-MEM or α-MEM supplemented with 15% FBS (fetal bovine serum), at 37°C in an atmosphere of 95% air and 5% CO_2, in 24-well plates to 80% confluence. All antibiotics were removed 24 h before infection with *Coxiella*.

Cell transfection

HeLa and CHO cells were transfected with the plasmids (1 mg ml^{-1}) using the LipofectAMINE 2000 reagent (Invitrogen, Argentina) according to the instructions supplied by the manufacturer. Transfected cells were incubated for 24 h in D-MEM supplemented with 15% FBS in 24 and 12-well plates to 80% confluence.

Propagation of C. burnetii *phase II*

Clone 4 phase II Nine Mile strain of *C. burnetii* bacteria, which are infective for cells but not for mammals, were provided by Ted Hackstadt (Rocky Mountain Laboratories, NIAID, NIH, Hamilton, MT, USA) and handled in a biosafety level II facility (Hackstadt, 1996). Infective inoculums were prepared as described (Zamboni *et al.*, 2001). Non-confluent Vero cells were cultured in T75 flasks at 37°C in D-MEM supplemented with 5% FBS, 0.22 g l^{-1} sodium bicarbonate and 20 mM Hepes, pH 7 (MfbH). Cultures were infected with *C. burnetii* phase II suspensions at 37°C in an air (CO$_2$) atmosphere. After 6 days, the cells were scrapped and passed 20 times through a 27-gauge needle connected to a syringe. Cell lysates were centrifuged at 1800 *g* for 10 min at 4°C. The supernatants were centrifuged at 25 000 *g* for 30 min at 4°C, and pellets containing *C. burnetii* were resuspended in D-MEM and passed 10 times through a 27-gauge needle connected to a syringe. Afterwards, the bacterial suspensions were aliquoted and kept frozen at −70°C.

Infection of cells with C. burnetii

HeLa and CHO cells plated in T25 flasks were washed two to three times with PBS and detached with trypsin-EDTA. After resuspension in D-MEM, cells were plated on coverslips distributed in 6-, 12- or 24-well plates. For infection, a 50 µl aliquot of *C. burnetii* suspension was diluted with 10 ml of D-MEM, and 0.5–1 ml of this dilution was added per well. In all experiments host cells were infected with *C. burnetii* at a multiplicity of infection (moi) of 10. Cells were incubated for different periods of time at 37°C in an atmosphere of 95% air and 5% CO$_2$.

Confocal microscopy

pEGFP-Vamp7 wt, pEGFP-Vamp7 NT, pEGFP-Vamp3, pEGFP-Vamp8 or pEGFP-transfected HeLa cells were analysed by confocal microscopy using an Olympus FluoViewTM FV1000 confocal microscope (Olympus, Argentina), with the FV10-ASW (version 01.07.00.16) software. Images were processed using Adobe CS3 (Adobe Systems).

Indirect immunofluorescence

HeLa and CHO cells were fixed with 3% paraformaldehyde solution in PBS for 10 min at room temperature, washed with PBS and blocked with 50 mM NH$_4$Cl in PBS. Subsequently, cells were permeabilized with 1% saponin in PBS containing 1% BSA, and then incubated with the primary antibody against *Coxiella* (1:1000). Bound antibodies were detected by incubation with a secondary antibody conjugated with Cy3 or Cy5 (1:800) (Jackson Immuno Research Laboratories, USA). Cells were mounted with Mowiol (plus Hoescht) and examined by confocal microscopy.

Measurement of the percentage of infected cells and the number and size of C. burnetii *RVs*

At different infection times, cells were fixed for 10 min in 3% paraformaldehyde. About 500 cells per coverslip (in triplicates) were scored for the presence or absence of large *C. burnetii* vacuoles using a confocal microscope (Olympus) with a 60× objective. Infected cells were defined as those with at least one large parasitophorous vacuole (size ≥ 2 µm) with clear identifiable bacteria inside. The size of the vacuoles was determined by a morphometric analysis using the FV10-ASW or ImageJ software.

siRNA silencing of Vamp7

Purified siRNA against human Vamp7 and control siRNA were purchased from BIONEER (Korea). Confluent HeLa cells were transfected with Vamp7 siRNA or with control siRNA, both prepared at a final concentration of 20 nM in 400 ml of opti-MEM without serum and with Lipofectamine 2000 reagent. The mix was added to a 24-well culture dish. After 5 h, the transfection mix was replaced by fresh D-MEM with 10% FBS. At 48 h post transfection the medium was removed and the same transfection protocol with the corresponding siRNA was applied again (second hit). When the second transfection mix was removed the HeLa cells were infected with *C. burnetii* for 72 h at 37°C.

Western blot

HeLa cells were washed twice, scraped and resuspended in sample buffer containing 1% 2-mercaptoethanol, and sonicated for 10 min at 4°C. For Western blot analysis, protein extracts were subjected to electrophoresis in 12.5% SDS-PAGE gels and transferred to a Hybond-enhanced chemoluminescence nitrocellulose membrane (Amersham) (GE, Buenos Aires, Argentina). Membranes were blocked with blotto (PBS with 5% non-fat milk and 0.1% Tween-20) for 1 h at room temperature. Subsequently, membranes were washed twice with PBS/Tween-20 0.1% and incubated with the primary antibody. To detect Vamp7, membranes were incubated overnight at 4°C with mouse anti-Vamp7 1:200 (abcam), washed and incubated with HRP-conjugated anti-mouse antibody (Jackson Immunoresearch Laboratories, USA), at a final dilution of 1:10 000. Equivalent protein loadings were confirmed by incubating membranes with a mouse anti-tubulin antibody (1:300) for 1 h at room temperature. The bands were visualized using the ECL reagent from GE, Buenos Aires, Argentina. Images of the bands were obtained using a Luminescent Image Analyser LAS-4000 (Fujifilm, Japan).

Fluorescent infectious focus-forming units experiment (FFU)

HeLa cells were plated in a six-well culture dish. After 24 h cells were washed with sterile PBS and co-transfected with pEGFP and a siRNA against Vamp7 or an irrelevant siRNA as negative

control. After 24 h, cells were infected with *C. burnetii* and following 24 h of infection the cells were transfected for a second time and cultured for an additional 24 h period to allow the development of the large *Coxiella* vacuole. After 48 h of infection the cells were scraped and lysed by sonication. Cell lysates with released *C. burnetii* were diluted (1:500) and used to infect Vero cells plated on a 12-well culture dish. After 72 h of incubation (chase), cells were fixed and mounted with Mowiol (plus Hoescht) and examined by fluorescence microscopy. The number of FFU per cell was analysed using the ImageJ software. Data represent the mean ± SEM of at least two independent experiments where at least 1000 cells were scored in each experiment.

Homotypic fusion assays

HeLa or CHO cells were plated at a confluence of 50–60% the day before the experiment. Cells were infected with *C. burnetii* (moi = 10) and after 24 h of infection cells were transfected with pEGFP-Vamp7 wt or pEGFP-Vamp7 NT. At 48 h of infection, cells were allowed to internalize mCherry-*Coxiella*. The 24 wells plate was centrifuged for 10 min (1500 r.p.m.) in order to induce the contact of the mCherry-*Coxiella* (red) to the cell surface. After 2 h of incubation cells were washed three times with PBS, fixed with 3% paraformaldehyde for 12 min and quenched with NH4Cl 50 mM for 15 min. Cells were subjected to indirect immunofluorescence using a polyclonal antibody against *C. burnetii*. The glass slides were mounted using Mowiol and analysed by confocal microscopy.

Heterotypic fusion assays

HeLa or CHO were plated at a confluence of 50–60% the day before the experiment. Cells were incubated with 5 μg ml^{-1} dextran-rhodamine for 2 h then transfected with pEGFP-Vamp7 wt or pEGFP-Vamp7 NT. After 24 h of transfection, cells were infected with *C. burnetii*. The 24-well plate was centrifuged for 10 min (1500 r.p.m.) in order to induce contact of the *C. burnetii* with the cell surface. After 2 h of incubation, cells were washed three times with PBS, fixed with 3% paraformaldehyde for 12 min and quenched with NH$_4$Cl 50 mM for 15 min. Cells were subjected to indirect immunofluorescence using a polyclonal antibody against *C. burnetii*. The glass slides were mounted using Mowiol and analysed by confocal microscopy.

Labelling with N-Rh-PE

The fluorescent phospholipid analogue N-Rh-PE was inserted into the plasma membrane. An appropriate amount of the lipid, stored in chloroform/methanol (2:1), was dried briefly under nitrogen and subsequently solubilized in absolute ethanol. This ethanolic solution was injected with a Hamilton syringe into serum free RPMI (1% v/v) while vigorously vortexing. The mixture was then added to the cells, which were then incubated for 60 min at 4°C. After this incubation period, the medium was removed, and the cells were extensively washed with cold PBS to get rid of excess unbound lipids. Labelled cells were cultured in complete RPMI medium under several conditions allowing the internalized lipid to reach the MVBs. After this incubation, cells were washed in PBS and immediately mounted on coverslips and analysed by confocal microscopy in order to label endocytic compartments at different times after internalization.

References

Advani, R.J., Yang, B., Prekeris, R., Lee, K.C., Klumperman, J., and Scheller, R.H. (1999) VAMP-7 mediates vesicular transport from endosomes to lysosomes. *J Cell Biol* **146:** 765–776.

Antonin, W., Dulubova, I., Arac, D., Pabst, S., Plitzner, J., Rizo, J., *et al.* (2002) The N-terminal domains of syntaxin 7 and vti1b form three-helix bundles that differ in their ability to regulate SNARE complex assembly. *J Biol Chem* **277:** 36449–36456.

Baumert, M., Maycox, P.R., Navone, F., De, C.P., and Jahn, R. (1989) Synaptobrevin: an integral membrane protein of 18,000 daltons present in small synaptic vesicles of rat brain. *EMBO J* **8:** 379–384.

Beare, P.A., Unsworth, N., Andoh, M., Voth, D.E., Omsland, A., Gilk, S.D., *et al.* (2009) Comparative genomics reveal extensive transposon-mediated genomic plasticity and diversity among potential effector proteins within the genus *Coxiella*. *Infect Immun* **77:** 642–656.

Beare, P.A., Sandoz, K.M., Omsland, A., Rockey, D.D., and Heinzen, R.A. (2011) Advances in genetic manipulation of obligate intracellular bacterial pathogens. *Front Microbiol* **2:** 97.

Bennett, M.K., Calakos, N., Kreiner, T., and Scheller, R.H. (1992) Synaptic vesicle membrane proteins interact to form a multimeric complex. *J Cell Biol* **116:** 761–775.

Bennett, M.K., Garcia-Arraras, J.E., Elferink, L.A., Peterson, K., Fleming, A.M., Hazuka, C.D., *et al.* (1993) The syntaxin family of vesicular transport receptors. *Cell* **74:** 863–873.

Beron, W., Gutierrez, M.G., Rabinovitch, M., and Colombo, M.I. (2002) *Coxiella burnetii* localizes in a Rab7-labeled compartment with autophagic characteristics. *Infect Immun* **70:** 5816–5821.

Campoy, E.M., Zoppino, F.C., and Colombo, M.I. (2011) The early secretory pathway contributes to the growth of the *Coxiella*-replicative niche. *Infect Immun* **79:** 402–413.

de Chastellier, C., Thibon, M., and Rabinovitch, M. (1999) Construction of chimeric phagosomes that shelter *Mycobacterium avium* and *Coxiella burnetii* (phase II) in doubly infected mouse macrophages: an ultrastructural study. *Eur J Cell Biol* **78:** 580–592.

Coleman, S.A., Fischer, E.R., Howe, D., Mead, D.J., and Heinzen, R.A. (2004) Temporal analysis of *Coxiella burnetii* morphological differentiation. *J Bacteriol* **186:** 7344–7352.

Colombo, M.I., Gutierrez, M.G., and Romano, P.S. (2006) The two faces of autophagy: *Coxiella* and *Mycobacterium*. *Autophagy* **2:** 162–164.

Delevoye, C., Nilges, M., Dautry-Varsat, A., and Subtil, A. (2004) Conservation of the biochemical properties of IncA

from *Chlamydia trachomatis* and *Chlamydia caviae*: oligomerization of IncA mediates interaction between facing membranes. *J Biol Chem* **279:** 46896–46906.

Delevoye, C., Nilges, M., Dehoux, P., Paumet, F., Perrinet, S., Dautry-Varsat, A., *et al.* (2008) SNARE protein mimicry by an intracellular bacterium. *PLoS Pathog* **4:** e1000022.

Fader, C.M., Sanchez, D.G., Mestre, M.B., and Colombo, M.I. (2009) TI-VAMP/VAMP7 and VAMP3/cellubrevin: two v-SNARE proteins involved in specific steps of the autophagy/multivesicular body pathways. *Biochim Biophys Acta* **1793:** 1901–1916.

Fasshauer, D. (2003) Structural insights into the SNARE mechanism. *Biochim Biophys Acta* **1641:** 87–97.

Fields, I.C., Shteyn, E., Pypaert, M., Proux-Gillardeaux, V., Kang, R.S., Galli, T., *et al.* (2007) v-SNARE cellubrevin is required for basolateral sorting of AP-1B-dependent cargo in polarized epithelial cells. *J Cell Biol* **177:** 477–488.

Flowerdew, S.E., and Burgoyne, R.D. (2009) A VAMP7/Vti1a SNARE complex distinguishes a non-conventional traffic route to the cell surface used by KChIP1 and Kv4 potassium channels. *Biochem J* **418:** 529–540.

Gaisano, H.Y., Sheu, L., Foskett, J.K., and Trimble, W.S. (1994) Tetanus toxin light chain cleaves a vesicle-associated membrane protein (VAMP) isoform 2 in rat pancreatic zymogen granules and inhibits enzyme secretion. *J Biol Chem* **269:** 17062–17066.

Galli, T., Chilcote, T., Mundigl, O., Binz, T., Niemann, H., and De, C.P. (1994) Tetanus toxin-mediated cleavage of cellubrevin impairs exocytosis of transferrin receptor-containing vesicles in CHO cells. *J Cell Biol* **125:** 1015–1024.

Galli, T., Zahraoui, A., Vaidyanathan, V.V., Raposo, G., Tian, J.M., Karin, M., *et al.* (1998) A novel tetanus neurotoxin-insensitive vesicle-associated membrane protein in SNARE complexes of the apical plasma membrane of epithelial cells. *Mol Biol Cell* **9:** 1437–1448.

Ghigo, E., Capo, C., Tung, C.H., Raoult, D., Gorvel, J.P., and Mege, J.L. (2002) *Coxiella burnetii* survival in THP-1 monocytes involves the impairment of phagosome maturation: IFN-gamma mediates its restoration and bacterial killing. *J Immunol* **169:** 4488–4495.

Gomes, M.S., Paul, S., Moreira, A.L., Appelberg, R., Rabinovitch, M., and Kaplan, G. (1999) Survival of *Mycobacterium avium* and *Mycobacterium tuberculosis* in acidified vacuoles of murine macrophages. *Infect Immun* **67:** 3199–3206.

Gutierrez, M.G., Vazquez, C.L., Munafo, D.B., Zoppino, F.C., Beron, W., Rabinovitch, M., *et al.* (2005) Autophagy induction favours the generation and maturation of the *Coxiella*-replicative vacuoles. *Cell Microbiol* **7:** 981–993.

Hackstadt, T. (1996) Biosafety concerns and *Coxiella burnetii*. *Trends Microbiol* **4:** 341–342.

Heinzen, R.A., Scidmore, M.A., Rockey, D.D., and Hackstadt, T. (1996) Differential interaction with endocytic and exocytic pathways distinguish parasitophorous vacuoles of *Coxiella burnetii* and *Chlamydia trachomatis*. *Infect Immun* **64:** 796–809.

Hong, W. (2005) SNAREs and traffic. *Biochim Biophys Acta* **1744:** 493–517.

Howe, D., and Mallavia, L.P. (2000) *Coxiella burnetii* exhibits morphological change and delays phagolysosomal fusion after internalization by J774A.1 cells. *Infect Immun* **68:** 3815–3821.

Howe, D., Shannon, J.G., Winfree, S., Dorward, D.W., and Heinzen, R.A. (2010) *Coxiella burnetii* phase I and II variants replicate with similar kinetics in degradative phagolysosome-like compartments of human macrophages. *Infect Immun* **78:** 3465–3474.

Humeau, Y., Doussau, F., Grant, N.J., and Poulain, B. (2000) How botulinum and tetanus neurotoxins block neurotransmitter release. *Biochimie* **82:** 427–446.

Jahn, R., and Scheller, R.H. (2006) SNAREs – engines for membrane fusion. *Nat Rev Mol Cell Biol* **7:** 631–643.

Martinez, I., Chakrabarti, S., Hellevik, T., Morehead, J., Fowler, K., and Andrews, N.W. (2000) Synaptotagmin VII regulates Ca(2+)-dependent exocytosis of lysosomes in fibroblasts. *J Cell Biol* **148:** 1141–1149.

Martinez-Arca, S., Rudge, R., Vacca, M., Raposo, G., Camonis, J., Proux-Gillardeaux, V., *et al.* (2003) A dual mechanism controlling the localization and function of exocytic v-SNAREs. *Proc Natl Acad Sci USA* **100:** 9011–9016.

Maurin, M., and Raoult, D. (1999) Q fever. *Clin Microbiol Rev* **12:** 518–553.

Maxfield, F.R., and McGraw, T.E. (2004) Endocytic recycling. *Nat Rev Mol Cell Biol* **5:** 121–132.

Mayorga, L.S., and Campoy, E.M. (2010) Modeling fusion/fission-dependent intracellular transport of fluid phase markers. *Traffic* **11:** 1001–1015.

Morozova, I., Qu, X., Shi, S., Asamani, G., Greenberg, J.E., Shuman, H.A., *et al.* (2004) Comparative sequence analysis of the *icm/dot* genes in *Legionella*. *Plasmid* **51:** 127–147.

Newton, H.J., and Roy, C.R. (2011) The *Coxiella burnetii* Dot/Icm system creates a comfortable home through lysosomal renovation. *MBio* **2:** e00226-11. doi: 10.1128/mBio.00226-11

Omsland, A., Cockrell, D.C., Howe, D., Fischer, E.R., Virtaneva, K., Sturdevant, D.E., *et al.* (2009) Host cell-free growth of the Q fever bacterium *Coxiella burnetii*. *Proc Natl Acad Sci USA* **106:** 4430–4434.

Oyler, G.A., Higgins, G.A., Hart, R.A., Battenberg, E., Billingsley, M., Bloom, F.E., *et al.* (1989) The identification of a novel synaptosomal-associated protein, SNAP-25, differentially expressed by neuronal subpopulations. *J Cell Biol* **109:** 3039–3052.

Polgar, J., Chung, S.H., and Reed, G.L. (2002) Vesicle-associated membrane protein 3 (VAMP-3) and VAMP-8 are present in human platelets and are required for granule secretion. *Blood* **100:** 1081–1083.

Proux-Gillardeaux, V., Rudge, R., and Galli, T. (2005) The tetanus neurotoxin-sensitive and insensitive routes to and from the plasma membrane: fast and slow pathways? *Traffic* **6:** 366–373.

Pryor, P.R., Mullock, B.M., Bright, N.A., Lindsay, M.R., Gray, S.R., Richardson, S.C., *et al.* (2004) Combinatorial SNARE complexes with VAMP7 or VAMP8 define different late endocytic fusion events. *EMBO Rep* **5:** 590–595.

Rao, S.K., Huynh, C., Proux-Gillardeaux, V., Galli, T., and Andrews, N.W. (2004) Identification of SNAREs involved in synaptotagmin VII-regulated lysosomal exocytosis. *J Biol Chem* **279:** 20471–20479.

Roberts, R.L., Barbieri, M.A., Pryse, K.M., Chua, M., Morisaki, J.H., and Stahl, P.D. (1999) Endosome fusion in living cells overexpressing GFP-rab5. *J Cell Sci* **112** (Part 21)**:** 3667–3675.

Romano, P.S., Gutierrez, M.G., Beron, W., Rabinovitch, M., and Colombo, M.I. (2007) The autophagic pathway is actively modulated by phase II *Coxiella burnetii* to efficiently replicate in the host cell. *Cell Microbiol* **9:** 891–909.

Siddiqi, S.A., Siddiqi, S., Mahan, J., Peggs, K., Gorelick, F.S., and Mansbach, C.M. (2006) The identification of a novel endoplasmic reticulum to Golgi SNARE complex used by the prechylomicron transport vesicle. *J Biol Chem* **281:** 20974–20982.

Sinai, A.P., Paul, S., Rabinovitch, M., Kaplan, G., and Joiner, K.A. (2000) Coinfection of fibroblasts with *Coxiella burnetti* and *Toxoplasma gondii*: to each their own. *Microbes Infect* **2:** 727–736.

Sollner, T., Bennett, M.K., Whiteheart, S.W., Scheller, R.H., and Rothman, J.E. (1993) A protein assembly-disassembly pathway *in vitro* that may correspond to sequential steps of synaptic vesicle docking, activation, and fusion. *Cell* **75:** 409–418.

Tayeb, M.A., Skalski, M., Cha, M.C., Kean, M.J., Scaife, M., and Coppolino, M.G. (2005) Inhibition of SNARE-mediated membrane traffic impairs cell migration. *Exp Cell Res* **305:** 63–73.

Turton, K., Chaddock, J.A., and Acharya, K.R. (2002) Botulinum and tetanus neurotoxins: structure, function and therapeutic utility. *Trends Biochem Sci* **27:** 552–558.

Veras, P.S., de Chastellier, C., Moreau, M.F., Villiers, V., Thibon, M., Mattei, D., *et al.* (1994) Fusion between large phagocytic vesicles: targeting of yeast and other particulates to phagolysosomes that shelter the bacterium *Coxiella burnetii* or the protozoan *Leishmania amazonensis* in Chinese hamster ovary cells. *J Cell Sci* **107** (Part 11)**:** 3065–3076.

Veras, P.S., Moulia, C., Dauguet, C., Tunis, C.T., Thibon, M., and Rabinovitch, M. (1995) Entry and survival of *Leishmania amazonensis* amastigotes within phagolysosome-like vacuoles that shelter *Coxiella burnetii* in Chinese hamster ovary cells. *Infect Immun* **63:** 3502–3506.

Vidal, M., Mangeat, P., and Hoekstra, D. (1997) Aggregation reroutes molecules from a recycling to a vesicle-mediated secretion pathway during reticulocyte maturation. *J Cell Sci* **110** (Part 16)**:** 1867–1877.

Walch-Solimena, C., Blasi, J., Edelmann, L., Chapman, E.R., von Mollard, G.F., and Jahn, R. (1995) The t-SNAREs syntaxin 1 and SNAP-25 are present on organelles that participate in synaptic vesicle recycling. *J Cell Biol* **128:** 637–645.

Zamboni, D.S., Mortara, R.A., and Rabinovitch, M. (2001) Infection of Vero cells with *Coxiella burnetii* phase II: relative intracellular bacterial load and distribution estimated by confocal laser scanning microscopy and morphometry. *J Microbiol Methods* **43:** 223–232.

Zamboni, D.S., McGrath, S., Rabinovitch, M., and Roy, C.R. (2003) *Coxiella burnetii* express type IV secretion system proteins that function similarly to components of the *Legionella pneumophila* Dot/Icm system. *Mol Microbiol* **49:** 965–976.

Zusman, T., Yerushalmi, G., and Segal, G. (2003) Functional similarities between the icm/dot pathogenesis systems of *Coxiella burnetii* and *Legionella pneumophila*. *Infect Immun* **71:** 3714–3723.

Supporting information

Additional Supporting Information may be found in the online version of this article:

Fig. S1. Vamp8 does not colocalize with Vamp7 in the fully developed CRVs.
A. Transiently transfected HeLa cells overexpressing pEGFP-Vamp8 were infected with *C. burnetii*. After 48 h of infection, the cells were fixed and subjected to a double indirect immunofluorescence using specific antibodies against Vamp7 (red) and *C. burnetii* (blue). The cells were analysed by confocal microscopy. Insets show no colocalization between endogenous Vamp7 and overexpressed Vamp8 on the *Coxiella* vacuole (see arrows).
B. HeLa cells were infected with *Coxiella burnetii*. After infection, the cells were fixed at different times (1 h, 6 h, 12 h 24 h and 48 h) and subjected to a double immunofluorescence using specific antibodies against *C. burnetii* (red) and Syntaxin1 (Stx1, green). The images show no-colocalization between *C. burnetii* and Stx1 at any tested times.
Fig. S2. Vti1a and Vti1b are recruited to the *Coxiella* phagosomes in a bacterial-dependent manner. *Coxiella burnetii* was pretreated with 100 μg ml^{-1} chloramphenicol for 30 min. After treatment, HeLa cells were infected with either control or chloramphenicol-pretreated *Coxiella,* maintaining the antibiotic in the culture medium, and fixed at different infection times (1 h, 6 h, 12 h and 24 h). After fixation the cells were subjected to a double immunofluorescence using specific antibodies against *C. burnetii* and Vti1a or Vti1b.
A. The bar graph shows that in cells that were treated with chloramphenicol the colocalization between endogenous Vti1a and *Coxiella* decreased significantly at all times analysed.
B. The bar graph shows that in cells that were treated with chloramphenicol the colocalization between endogenous Vti1a and *Coxiella* decreased significantly at all times analysed.
Fig. S3. Overexpression of EGFP-Vamp7 wt or EGFP-Vamp7 NT does not affect *Coxiella* internalization in HeLa cells. HeLa cells were transfected with pEGFP-Vamp7 wt or pEGFP-Vamp7 NT. After 24 h of transfection the cells were infected with *C. burnetii* for 2 h in a multiplicity of infection of 10 (A) or 20 (B), fixed and subjected to indirect immunofluorescence using a specific antibody against *C. burnetii*.
Fig. S4. Overexpression of the tetanus toxin does not affect the homotypic and heterotypic fusion capacity of the CRVs.
A. HeLa cells transiently transfected with EGFP-Vamp3 wt or cells transiently co-transfected with EGFP-Vamp3 wt and TeNT were infected with *Coxiella burnetii*. At 2 h of infection, cells were fixed and subjected to a double immunofluorescence using specific antibodies against CD63 (LAMP 3) and *C. burnetii*. The cells were analysed by confocal microscopy. Quantification of the colocalization between *C. burnetii* and CD63 shows a nonsignificant decrease in the percentage of colocalization in cells overexpressing the tetanus toxin compared with the control condition. Data represent the mean ± SEM of at least two independent experiments.
B. HeLa cells were infected with *C. burnetii* for 24 h and transfected with pEGFP-Vamp7 wt or pEGFP-Vamp7 NT. After

24 h of transfection, cells were infected with mCherry *Coxiella* for 2 h, fixed and subjected to indirect immunofluorescence using specific antibodies against *C. burnetii*. The cells were analysed by confocal microscopy. Quantification of the colocalization between *C. burnetii* and mCherry-*Coxiella*. The bar graph shows non-significant differences in the percentage of colocalization under TeNT overexpression compared with the control.

Fig. S5. *In vivo* analysis of homotypic fusion between *Coxiella* vacuoles in cells overexpressing EGFP-Vamp8.

A. HeLa cells transiently overexpressing EGFP-Vamp8 were infected with *C. burnetii* (moi = 10). After 24 h the cells were mounted into an *in vivo* camera and analysed by confocal microscopy for 42 min.

B. Inset showing the final stage of the fusion. C. Insets of the experiment described in A, showing the sequences of the movie (every 5 min). Red arrows indicate the CRVs, white arrows point to the fusion site.

Movie S1. Homotypic fusion between *C. burnetii* vacuoles in cells overexpressing EGFP-Vamp7 overexpression. HeLa cells transiently overexpressing EGFP-Vamp7 wt were infected with *C. burnetii* (moi = 10). After 24 h the cells were mounted into an *in vivo* camera and analysed by confocal microscopy for 70 min. The arrow indicates the marked enrichment of Vamp7 at the docking and fusion site.

Movie S2. Homotypic fusion between *C. burnetii* vacuoles in cell overexpressing EGFP-Vamp8 overexpression. HeLa cells transiently overexpressing EGFP-Vamp8 were infected with *C. burnetii* (moi = 10). After 24 h the cells were mounted into an *in vivo* camera and they were analysed by confocal microscopy for 42 min. The arrow points to the fusion site. No accumulation of Vamp8 is observed.